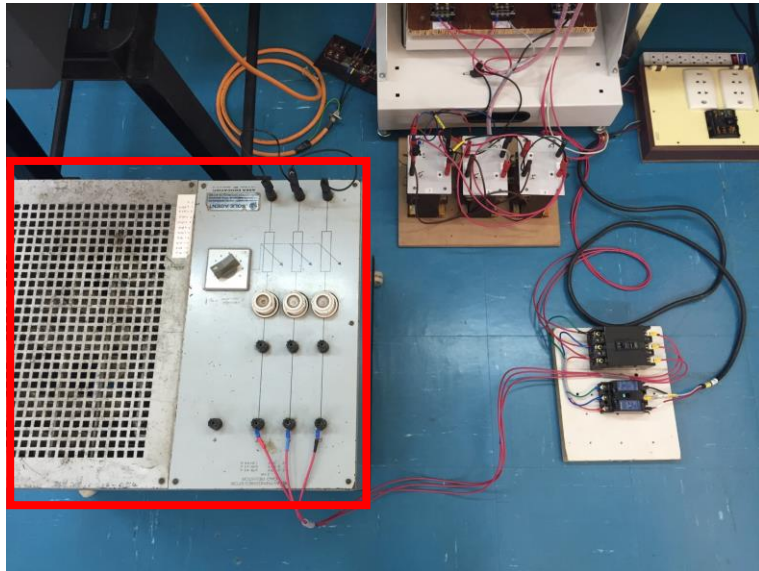
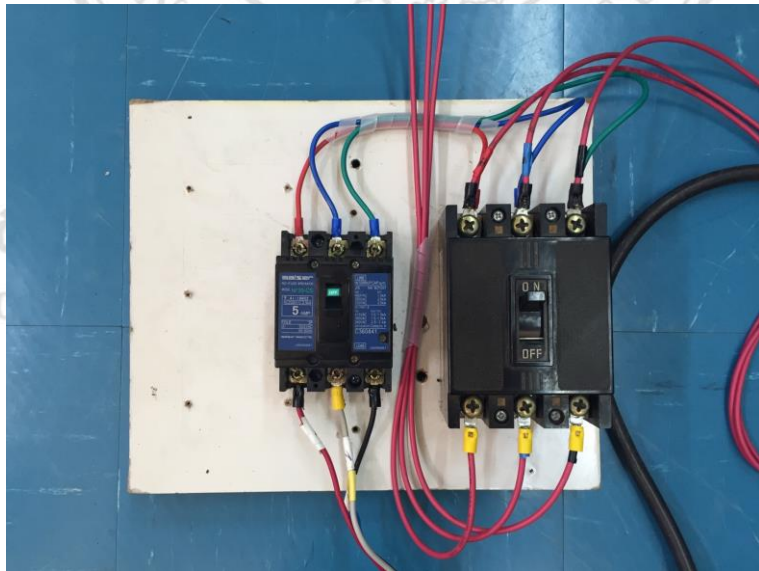


## ภาคผนวก ก

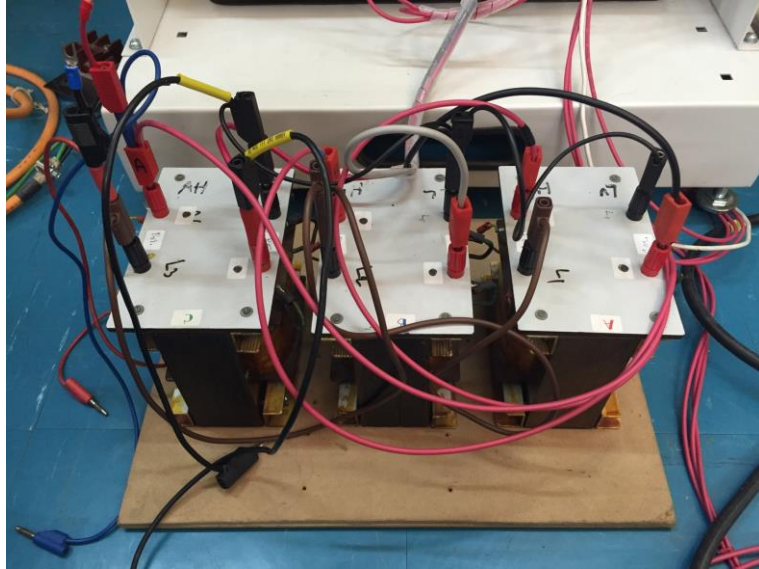
### อุปกรณ์ที่ใช้ในการทำวิจัย



ภาพที่ ก.1 ตัวต้านทานสามเฟสขนาด 5 กิโลวัตต์ (วงกลมแดง)



ภาพที่ ก.2 เบรกเกอร์สามเฟส สำหรับโหลดตัวต้านทาน และกริดไฟฟ้า



ภาพที่ ก.3 หม้อแปลงแยกขดสามเฟส 1/4



ภาพที่ ก.4 ตัวเหนี่ยวนำสามเฟส

ลิขสิทธิ์ © by Chiang Mai University  
All rights reserved

ภาคผนวก ข

งานวิจัยที่ได้รับการเผยแพร่



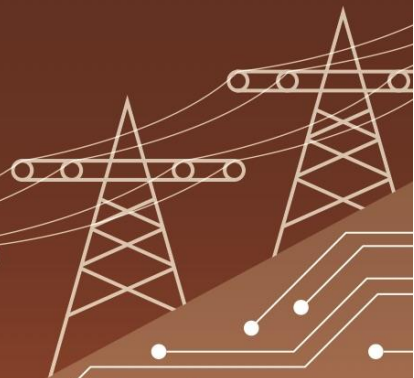
ลิขสิทธิ์มหาวิทยาลัยเชียงใหม่  
Copyright© by Chiang Mai University  
All rights reserved



2013 10th International Conference on  
Electrical Engineering/Electronics, Computer,  
Telecommunications and Information Technology

# ECTI-CON 2013

Krabi, Thailand  
May 15-17, 2013



ISBN : 978-1-4799-0545-4  
IEEE catalog number : CFP1306E-ART





# Performance Enhancement of PMSG Systems with Control of Generator-side Converter Using $d$ -axis Stator Current Controller

K. Bunjongjit, Y. Kumsuwan

Department of Electrical Engineering Faculty of Engineering, Chiang Mai University, Chiang Mai 50200, Thailand  
yt@eng.cmu.ac.th

**Abstract**— This paper presents a performance enhancement of a permanent magnet synchronous generator (PMSG) system with control of generator-side converter for a wind turbine application. This method uses zero  $d$ -axis stator current control to minimize winding losses of the generator. The electromagnetic torque of the generator is correlated with the magnitude of the  $q$ -axis stator current, while the  $d$ -axis stator current is regulated at zero, the control scheme decouples  $dq$ -axis stator current control through vector control for the generator-side converter. This paper also presents mathematical analysis of the active power and stator power factor, and the maximum power point tracking (MPPT) operation. Simulation results are provided to guarantee the proposed control scheme, in which the performance enhancement and efficiency.

**Keywords**— Permanent-magnet synchronous generator (PMSG); wind generation; generator-side control; maximum power point tracking (MPPT);  $d$ -axis stator current control.

## I. INTRODUCTION

Over the recent years, wind energy has been considered as one of the most significant renewable energy sources. Among the existing wind power generation systems, its generators can be categorized into four main types [1], [2]: 1) doubly fed induction generator 2) squirrel cage induction generator 3) wound rotor synchronous generator and 4) permanent magnet synchronous generator. Nowadays, wind energy industry uses PMSG for direct grid-connection because it gives higher efficiency and has no slip ring maintenance. Thus, the lightweight and low maintenance features can be obtained in this type of wind power generation system [3], [4].

The configuration of PMSG wind power generation system is shown in Fig. 1. Presently, there are a few papers examined for the generator-side wind power generation control [5]-[7]. For this reason, this paper focuses on the analysis of generator-side converter  $d$ -axis stator current control approaches for control of PMSG wind turbines. The generator-side can be controlled with various schemes, the control schemes are separated into three control strategy types to execute different intentions: 1) zero  $d$ -axis stator current (ZDSC): control to achieve a linear relationship between the stator current and generator torque 2) maximum torque per-ampere (MTPA): control to produce maximum generator torque with a minimum stator current and 3) unity power factor (UPF): control to maintain power factor at one.

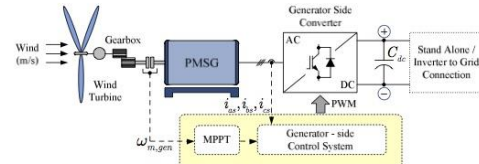


Fig. 1. Configuration of PMSG system with control of generator-side converter using  $d$ -axis stator current control scheme.

However, there are other techniques for the generator-side control presented in [5]-[6], namely, a vector control. The control strategy in the generator-side has two control loops, three PI controllers and many measured variables from generator-side and grid-side which leads to seriously complicate control design. Compared with the proposed control strategy in [7], ZDSC control can provide a simple topology solution and excellent generator integration performance such as a simple control algorithm, generate maximum efficiency, and minimize system losses. However, the major drawback of ZDSC control is not suitable for salient-pole synchronous generators and it is not optimal for the operation range over the base speed.

The main objective of this paper is to describe the generator-side performance using ZDSC control scheme. The wind turbine PMSG generation system operates in the base speed range. The dynamic equations of the PMSG and ZDSC control scheme are analyzed in a space vector diagram and phasor diagram, respectively. The stator power factor and the generator active power are discussed. Furthermore, comparison between the generator active power and the mechanical power are studied to establish a performance enhancement for the system. Additionally, the MPPT method is implemented which can provide the optimal torque control along the whole operation range. Simulation results are shown to verify the performance of the proposed control strategy for PMSG generation system.

## II. PRINCIPLES OF THE PMSG WIND ENERGY SYSTEM

The configuration of PMSG wind power generation system is shown in Fig. 1. The PMSG converts the mechanical power from the wind turbine into ac electrical power, which is then converted to dc power through a converter with dc link supplying either to the stand-alone load or the inverter to grid-connection. By using an additional inverter, the PMSG can

supply the ac electrical power with constant voltage and frequency to the power grid. Two control functions are implemented on the generator-side: one is to extract maximum power available from the wind turbine and the other is to optimize generator operation, which will be discussed in the following.

#### A. Maximum Power Point Tracking (MPPT) with Optimal Torque Control

The mechanical torque  $T_m$ , which is captured by a wind turbine, can be expressed as [8]

$$T_m = \frac{1}{2} \rho A v_w^3 C_p / \omega_m r_t \quad (1)$$

where  $\rho$  is the air density,  $A$  is the sweep area of the wind turbine,  $v_w$  is the wind velocity,  $r_t$  is the turbine radius,  $\omega_m$  is the generator speed, and  $C_p$  is the power coefficient of the wind turbine.

From (1), in order to capture the maximum mechanical power from a wind turbine at different wind speeds, see the wind turbine power-speed characteristics and maximum power point operation that are shown in Fig. 2. It can be seen that the trajectory of the black circles represents a MPPT power curve, which can be expressed in term of the mechanical torque  $T_{m,MPPT}$  by the following equations

$$T_{m,MPPT} = K_{opt} \omega_m^2 \quad (2)$$

where  $K_{opt}$  is the coefficient for the optimal torque, which can be calculated according to the rated parameters of the generator.

Equation (2) shows the relationship between the generator speed  $\omega_m$  and mechanical torque  $T_{m,MPPT}$  of the wind turbine that can be used to determine the optimal torque reference to control the generator-side converter and achieve the MPPT method operation. Otherwise, the maximum power operation can also be achieved with optimal torque control.

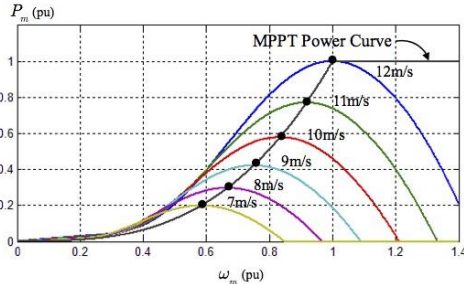


Fig. 2. Wind turbine power-speed characteristic and maximum power point tracking (MPPT) method operation.

#### B. Dynamic Model of PMSG

In order to get a dynamic model for the PMSG that easily allows us to define the generator-side control system. Fig. 3 shows an arbitrary  $dq$ -axis dynamic model of PMSG in the rotor field synchronous reference frame.

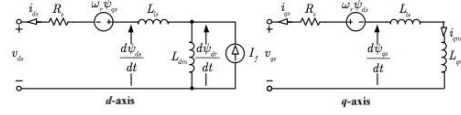


Fig. 3. Arbitrary  $dq$ -axis dynamic model of the PMSG in the rotor field synchronous reference frame ( $dq$ -axis).

The voltage equations of the PMSG are given by

$$v_{ds} = - \left( R_s i_{ds} + L_d \frac{di_{ds}}{dt} \right) + \omega_r L_q i_{qs} \quad (3)$$

$$v_{qs} = - \left( R_s i_{qs} + L_q \frac{di_{qs}}{dt} \right) - \omega_r L_d i_{ds} + \omega_r \vec{\psi}_r \quad (4)$$

where  $R_s$  is the PMSG stator resistance,  $\vec{\psi}_r$  is the rotor flux-linkages,  $L_d$  and  $L_q$  are the stator  $dq$ -axis self-inductances,  $i_{ds}$  and  $i_{qs}$  are the  $dq$ -axis stator currents, and  $\omega_r$  is rotor speed.

The generator torque  $T_e$  of the PMSG can be calculated by

$$T_e = \frac{3p_p}{2} \left[ \vec{\psi}_r i_{qs} - (L_d - L_q) i_{ds} i_{qs} \right] \quad (5)$$

where  $p_p$  is the pole pairs.

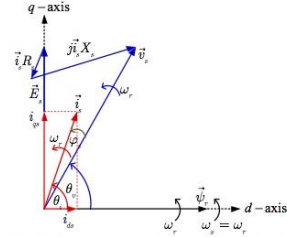


Fig. 4. A space vector diagram of the PMSG

Following the arbitrary  $dq$ -axis dynamic model of the PMSG in Fig. 3, a space vector diagram for the PMSG is expressed in Fig. 4. The space vector diagram is derived under the rotor flux-linkage which is aligned with the  $d$ -axis of the synchronous reference frame. All vectors in this diagram together with  $dq$ -axis frame rotate in space at the synchronous speed, which is also the rotor speed of the generator  $\omega_r$ .

### III. CONTROL OF THE GENERATOR-SIDE CONVERTER

#### A. Zero $d$ -Axis Stator Current (ZDSC) Control

The proposed generator-side control scheme is shown in Fig. 5. MPPT and ZDSC controls are implemented on the



generator-side. The generator torque reference  $T_e^*$  is generated by the MPPT method in agreement with the measured generator speed  $\omega_m$ . The generator torque reference produces  $q$ -axis stator current reference  $i_{qs}^*$ . The  $d$ -axis generator current reference  $i_{ds}^*$  is set according to the generator operation requirements. The measurement of the three-phase stator currents  $i_{as}, i_{bs}, i_{cs}$  are transformed into  $dq$ -axis stator currents  $i_{ds}, i_{qs}$  according to the measured rotor flux angle  $\theta_r$ . The measured  $dq$ -axis stator currents are subtracted with their current reference. The errors are sent to PI controllers which led to obtaining the  $dq$ -axis reference voltages  $v_{ds}^*, v_{qs}^*$  for the converter. The  $dq$ -axis reference voltage  $v_{ds}^*, v_{qs}^*$  are transformed into three-phase reference voltages  $v_{as}^*, v_{bs}^*, v_{cs}^*$  and sent to the PWM generation block using SVM modulation. The proposed generator-side control in more detail will be discussed in the following.

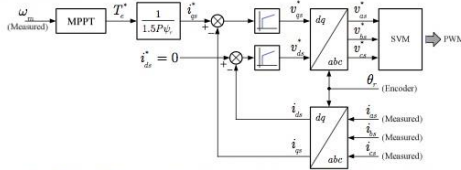


Fig. 5. Block diagram of the generator-side control algorithm based on zero  $d$ -axis stator current control scheme.

Zero  $d$ -axis stator current control is applied to improve the efficiency of the machine. With this control, the  $d$ -axis stator current component  $i_{ds}$  is then controlled to be zero ( $i_{ds} = 0$ ) to minimize generator current and thereby reducing the winding losses. With the  $d$ -axis stator current kept at zero, the stator current is equal to its  $q$ -axis component  $i_{qs}$ .

$$i_s = \sqrt{(i_{ds})^2 + (i_{qs})^2} = i_{qs} \quad (6)$$

According to the ZDSC Control scheme, the generator torque  $T_e$  from (5) can be simplified to

$$T_e = \frac{3}{2} p \psi_r i_{qs} = \frac{3}{2} p \psi_r i_s \quad (7)$$

Thus, the  $q$ -axis stator current reference  $i_{qs}^*$  can be determined as the following

$$i_{qs}^* = \frac{T_e^*}{1.5 p \psi_r} \quad (8)$$

Considering the relation stated on (7) and (8), the generator torque generated the  $q$ -axis stator current reference and the generator torque can also be controlled directly by the  $q$ -axis stator current. Furthermore, the  $dq$ -axis reference voltages for the converter can be derived from (3) and (4) as

$$v_{ds}^* = v_{ds}' + \omega_r L_q i_{qs}^* \quad (9)$$

$$v_{qs}^* = v_{qs}' - \omega_r L_d i_{ds}^* + \omega_r \hat{\psi}_r \quad (10)$$

The  $dq$ -axis reference voltages  $v_{ds}', v_{qs}'$  are sent to PWM generation block for generated PWM signals, as it was mentioned in the previous paragraph.

### B. ZDSC Control Performance Analysis

In order to analyse the performance of the ZDSC control, the control strategy was discussed based on the steady state condition, from (3) and (4), the steady-state voltage equations of the PMSG can be expressed as the following

$$V_{ds} = -R_s I_{ds} + \omega_r L_q I_{qs} \quad (11)$$

$$V_{qs} = -R_s I_{qs} - \omega_r L_d I_{ds} + \omega_r \hat{\psi}_r \quad (12)$$

From (11) and (12), they can be analysed into the phasor diagram to provide the control strategy analysis.

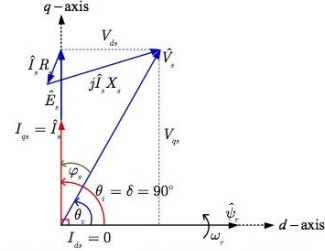


Fig. 5. A phasor diagram of the PMSG with ZDSC control.

Fig. 5 gives the ZDSC control phasor diagram in the synchronous reference frame, the stator power factor angle  $\varphi_s$  is define by

$$\varphi_s = \theta_i - \theta_v \quad (13)$$

where  $\theta_v$  and  $\theta_i$  are the stator voltage angle and the stator current angle, respectively.

As shown in Fig. 5, the ZDSC controls the stator current vector, which should always be kept aligned with the back EMF and perpendicular to the rotor flux-linkage of the PMSG. In other words, the stator current angle  $\theta_i$  or torque angle  $\delta$  should be set as  $90^\circ$ .

$$\theta_i = \delta = 90^\circ \quad (14)$$

The stator voltage angle  $\theta_v$  can be defined from Fig. 5. It can be explained by using the steady-state voltage equations from (11) and (12) as

$$\theta_v = \sin^{-1} \left( \frac{V_{qs}}{\sqrt{(V_{ds})^2 + (V_{qs})^2}} \right) = \sin^{-1} \frac{1}{\sqrt{1 + \frac{(L_d \hat{I}_s / \hat{\psi}_r)^2}{(1 + R_s \hat{I}_s / \omega_r \hat{\psi}_r)^2}}} \quad (15)$$

Substituting (14) and (15) into (13), the stator power factor angle  $\varphi_s$  equation with ZDSC control can be expressed as

$$\varphi_s = 90^\circ - \sin^{-1} \frac{1}{\sqrt{1 + \frac{(L_s \hat{I}_s / \hat{\psi}_r)^2}{(1 + R_s \hat{I}_s / \omega_r \hat{\psi}_r)^2}}} \quad (16)$$

Based on (16), when the stator inductance, resistance and rotor flux-linkage of PMSG are constant, the stator power factor angle  $\varphi_s$  under ZDSC control decomposes increasing stator current  $\hat{I}_s$  and rotor speed  $\omega_r$ , respectively. Consequently, when the stator power factor  $\text{PF}_s$  is low, the performance of the PMSG drive will be reduced by the increased apparent power  $S$  for producing the generator torque  $T_e$  and increasing the winding losses.

Considering the generator active power  $P_s$  of the PMSG under ZDSC control, it is expressed as

$$\begin{aligned} P_s &= 3 \cdot \frac{\sqrt{V_{ds}^2 + V_{qs}^2}}{\sqrt{2}} \cdot \frac{\sqrt{I_{ds}^2 + I_{qs}^2}}{\sqrt{2}} \cdot \text{PF}_s \\ &= 3 \cdot V_s \cdot I_s \cdot \cos(\varphi_s) \end{aligned} \quad (17)$$

where  $V_s$  and  $I_s$  are the rms voltage and phase current. Stator power factor angle  $\varphi_s$  can be calculated by (16) with the PMSG parameters.

From (17), the relationship between generator active power  $P_s$  and stator power factor  $\text{PF}_s$  can be obtained. The generator active power is reduced when the stator power factor is deteriorated.

#### IV. SIMULATION RESULTS

The performance enhancement of PMSG systems with control of generator-side converter using  $d$ -axis stator current control strategy (Fig. 1) was simulated in the Matlab/Simulink software for a wind generation system. The PMSG parameters are given in Table I. The simulation results are shown in Figs. 7-9.

TABLE I  
PERMANENT MAGNET SYNCHRONOUS GENERATOR PARAMETERS

| Permanent Magnet Synchronous Generator Parameters |               |          |
|---|---------------|----------|
|   |               | Per-unit |
| Rated Mechanical Power                            | 2.448 MW      | 1.0      |
| Rated Apparent Power                              | 3.419 MVA     | 1.0      |
| Rated Phase Voltage                               | 2309.4 V(rms) | 1.0      |
| Rated Stator Current                              | 490 A(rms)    | 1.0      |
| Rated Stator Frequency                            | 53.33 Hz      | 1.0      |
| Rated Rotor Speed                                 | 400 rpm       | 1.0      |
| Number of Pole Pairs                              | 8             |          |
| Rated Mechanical Torque                           | 58.459 kN.m   | 1.0      |
| Rated Rotor Flux-Linkage                          | 4.971 Wb(rms) | 0.7213   |
| Stator Winding Resistance                         | 24.21 mΩ      | 0.0052   |
| $d$ -Axis Stator Self-Inductance                  | 9.816 mH      | 0.7029   |
| $q$ -Axis Stator Self-Inductance                  | 9.816 mH      | 0.7029   |

In order to simulate the transient response of the proposed control system, Fig. 7 shows the simulated waveforms during the start-up of the PMSG wind turbine system. Generator speed  $\omega_m$  is assumed to have a ramp start-up from 0 pu at 0.1s to base speed at 1s as shown in Fig. 7(a). The transient

waveforms of the stator voltage (phase  $a$ )  $v_{sa}$ , stator currents  $i_s$  and  $dq$ -axis stator currents  $i_{ds}, i_{qs}$ , are shown in Fig. 7(b) and (c), respectively. With connecting to the stand alone resistive load, the waveforms of stator voltage become the switching pulse due to the switching effect of the inverter. In contrast, the waveform of the stator currents has been filtered through the inverter impedance and according to the high switching frequency of the inverter, stator currents are smoothing sinusoidal. The generator torque  $T_e$  starts to ramps up and follows to the optimal reference torque  $T_e^*$  for MPPT up to the base value, and the kept constant is shown in Fig. 7(d). With the ZDSC control scheme, the  $d$ -axis stator current is kept at zero and the response of the  $q$ -axis stator current doesn't affect the  $d$ -axis stator current response. In addition, the  $q$ -axis stator current is proportional to the generator torque.

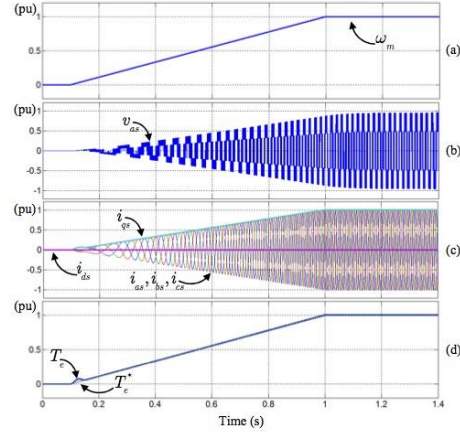


Fig. 7. Simulation results of the PMSG with ZDSC control scheme under ramp-startup condition. (a) generator speed, (b) phase stator voltage, (c)  $dq$ -axis stator currents and phase stator currents, and (d) generator torque.

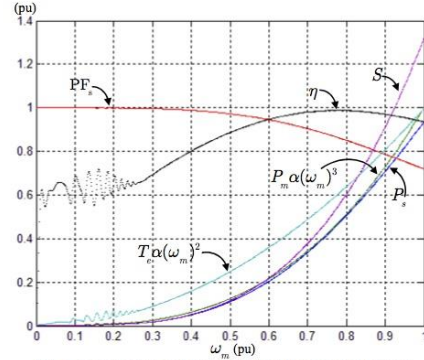


Fig. 8. Performance of the PMSG with ZDSC control scheme under start-up condition.



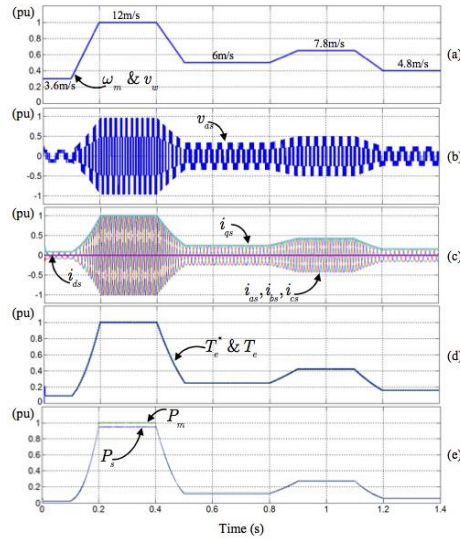


Fig. 9. Simulation results of the PMSG with ZDSC control scheme under wind speed step changes condition. (a) wind and rotor speed, (b) phase stator voltage, (c)  $dq$ -axis stator currents and phase stator currents, (d) generator torque, and (e) generator active power and mechanical power.

Fig. 8 shows the performance of the PMSG with the purposed control scheme under start-up condition. When the generator speed  $\omega_m$  increases to 0.8 pu, the PMSG reaches 0.99 pu efficiency  $\eta$  and slightly fall to 0.95 pu while the generator speed increases to base speed. In contrast, the stator power factor  $PF_s$  showed different changes by decreasing steadily from 1 pu to 0.71 pu. According to the increasing of the appearance power  $S$  to compensate the generator torque  $T_e$  and active power  $P_g$  around base speed range, reducing of the PMSG efficiency is occurring at the same time.

Fig. 9 shows the simulated waveforms of the PMSG during the wind speed  $v_w$  step change. Wind speed is assumed to have a step-up from 3.6 m/s to 12 m/s at 0.1s and fell sharply to 6 m/s at 0.5sec and then have a slight rise reaching around 7.8 m/s at 0.9s. Lastly, wind speed decreased steadily to 4.8 m/s at 1s then remained stable as shown in Fig. 9(a). In the other hand the wind speed is proportional to the generator speed according to a gearbox ratio. Fig. 9(b) and (c) shows the transient waveforms of the stator voltage (phase  $a$ ), stator currents and  $dq$ -axis stator currents, respectively. Fig. 9(d) shows the optimal reference torque for MPPT and the generator torque. The generator torque follows the optimal reference torque very well in transient and steady state.

The transient of the mechanical power  $P_m$  and generator active power  $P_g$  are shown in Fig. 9(e). At the instant time when the wind speed steps up, the MPPT operation gives the demand for generator torque to increase. The increase of

generator torque leads to higher mechanical power output. As the speed rises up to base speed, the generator's active power increases as well. The generator's active power reaches high point at 0.95 pu. It's reduced by the winding loss in a machine for 5% (0.05 pu) losses. In contrast, during wind speed step down transient, the generator's active power fall accordingly and keep constant in steady state. The mechanical power and the generator's active power almost have the same value, due to a very small winding loss in a machine. Consequently, it is verified that the proposed control scheme can realize high efficiency performance from 0 pu to base speed range, especially in the mid-operation range.

## V. CONCLUSIONS

In this paper, a performance enhancement of PMSG systems with control of the generator-side converter using  $d$ -axis stator current controller has been proposed and its performance was analyzed. The control strategy was developed for the optimize generator operation while extracting the maximum power from wind. The proposed control system decouples  $d$ -axis and  $q$ -axis stator current control through vector control for the generator-side converter. Particularly, the generator current was minimized to reduce the machine winding losses for achieving maximum overall performance and efficiency. The operating principle and theoretical analysis were verified using simulation results that exhibited improved high performance and high efficiency.

## ACKNOWLEDGMENT

The work was supported by the Faculty of Engineering, Chiang Mai University.

## REFERENCES

- [1] Z. Chen, J. M. Guerrero, and F. Blaabjerg, "A review of the state of the art of power electronics for wind turbines," *IEEE Trans. Power Electron.*, vol. 24, no. 8, pp. 1859-1875, Aug. 2009.
- [2] J. M. Carrasco, L. G. Franquelo, J. T. Biala siewicz, E. Galvan, R. C. P. Guisado, A.M. Parts, J. I. Leon, and N. Moreno-Alfonso, "Power-electronic systems for the grid integration of renewable energy sources: A survey," *IEEE Trans. Ind. Electron.*, vol. 53, no. 4, pp. 1002-1016, Aug. 2006.
- [3] A. Grauers, "Efficiency of three wind energy generator systems," *IEEE Trans. Energy Convers.*, vol. 11, no. 3, pp. 650-657, Sep. 1996.
- [4] Z. Chen and E. Spooner, "Wind turbine power converters: a comparative study," in *Proc. 1998 IEE Power Electronics and Variable Speed Drives Seventh International Conference*, pp. 471-476.
- [5] M. Chinchilla, S. Arnaltes, and J. C. Burgos, "Control of permanent-magnet generators applied to variable-speed wind-energy systems connected to the grid" *IEEE Trans. Energy Convers.*, vol. 21, no. 1, pp. 130-135, Mar. 2006.
- [6] K. Huang, S. Huang, F. She, B. Luo, and L. Cai, "A control strategy for direct-drive permanent-magnet wind-power Generator using back-to-back PWM converter" *ICEMS Conference*, pp. 2283-2288, Oct. 2008.
- [7] S. Zhang, K. Tseng, D. Mahinda Vilathgamuwa, and T. D. Nguyen, "Design of a robust grid interface system for PMSG-based wind turbine generators" *IEEE Trans. Ind. Electron.*, vol. 58, no. 1, pp. 316-328, Jan. 2011.
- [8] E. Koutroulis and K. Kalaitzakis, "Design of a maximum power tracking system for wind-energy-conversion applications," *IEEE Trans. Ind. Electron.*, vol. 53, no. 2, pp. 486-494, Apr. 2006.





## Vol 11, No 2 (2013)

### Regular Issue

### Table of Contents

#### Electrical Power Systems

|   |        |
|---|--------|
| <a href="#">Novel Circuit Breaker Modeling in 275kV Substation</a>  | PDF    |
| <i>Hamid Radmanesh, Razieh Salimi Atani</i>   | 1-7    |
| <a href="#">Transfer Function Analysis to Evaluate Drying Quality of Power Transformers by Support Vector Machine</a>                                     | PDF    |
| <i>Mehdi Bigdelli, Hormatollah Firoozi</i>  | 8-15   |
| <a href="#">Optimal DC Allocation in a Smart Distribution Grid Using Cuckoo Search Algorithm</a>  | PDF    |
| <i>Wirote Buaklee, Komsan Hongesombut</i>   | 16-22  |
| <a href="#">Robust Interline Power Flow Controller with Wind Power Source Using Phase-Plane Fuzzy Logic Control</a>                                       | PDF    |
| <i>Komsan Hongesombut, Thongchart Kerdphol</i>  | 23-27  |
| <a href="#">Determination of the Optimal Battery Capacity of a Grid-connected Photovoltaic System with Power and Frequency Fluctuations Consideration</a> | PDF    |
| <i>Chattrin Thongsawaeng, Kulyos Audomvongseree</i>   | 28-37  |
| <a href="#">Chirality (n, m) Dependence of Band Gap of Semiconducting SWCNT</a>   | PDF    |
| <i>G. R. Ahmed Jamal</i>  | 38-42  |
| <a href="#">Operational Amplifier Gain-Bandwidth Product Enhancement Technique for Common-mode Active EMI Filter Compensation Circuits</a>                | PDF    |
| <i>Vuttipon Tarateeraseth</i>   | 43-50  |
| <a href="#">Performance Enhancement of PMSG Systems with Control of Generator-side Converter Using d-axis Stator Current Controller</a>                   | PDF    |
| <i>Kitsanu Bunjongjit, Yuttana Kumsuwan</i>   | 51-57  |
| <a href="#">Dependable Capacity Evaluation of Wind Power and Solar Power Generation Systems</a>   | PDF    |
| <i>Chatbordin Naksrisuk, Kulyos Audomvongseree</i>  | 58-66  |
| <a href="#">Multi-Objective Design for Switched Reluctance Machines Using Genetic and Fuzzy Algorithms</a>  | PDF    |
| <i>Satit Owatthaiphong, Nisai Fuengwarodsakul</i>   | 67-78  |
| <a href="#">Design of Cogeneration and Analysis of Economic and Environmental Optimal Operations for Building Energy Management System</a>                | PDF    |
| <i>Thanakorn Petkajee, David Banjerdpongchai</i>  | 79-94  |
| <a href="#">Bat Optimization for a Dual-Source Energy Management in an Electric Vehicle Energy Storage Strategy</a>                                       | PDF    |
| <i>Boumediène Allaoua, Abdellah Laou, Brahim Mebarki</i>  | 95-100 |

#### USER

Username   
 Password   
 Remember me

#### JOURNAL CONTENT

Search   
 Search Scope  
 All

#### Browse

- [By Issue](#)
- [By Author](#)
- [By Title](#)

#### INFORMATION

- [For Readers](#)
- [For Authors](#)
- [For Librarians](#)

# Performance Enhancement of PMSG Systems with Control of Generator-side Converter Using d-axis Stator Current Controller

Kitsanu Bunjongjit\*<sup>1</sup>, Non-member and Yuttana Kumsuwan\*<sup>2</sup>, Member

## ABSTRACT

This paper presents a performance enhancement of a permanent magnet synchronous generator (PMSG) system with control of generator-side converter for a wind turbine application. This method uses zero d-axis stator current control to minimize winding losses of the generator. The electromagnetic torque of the generator is correlated with the magnitude of the q-axis stator current, while the d-axis stator current is regulated at zero, the control scheme decouples the dq-axis stator current control through a vector control for the generator-side converter. This paper also presents mathematical analysis of the active power and stator power factor, and the maximum power point tracking (MPPT) operation. Simulation results are provided to guarantee the proposed control scheme, in which the performance enhancement and efficiency are evaluated.

**Keywords:** Permanent-Magnet Synchronous Generator (PMSG), Wind Generation, Generator-side Control, Maximum Power Point Tracking (MPPT), D-axis Stator Current Control.

## 1. INTRODUCTION

Over recent years, wind energy has been considered as one of the most significant renewable energy sources. Among the existing wind power generation systems, its generators can be categorized into four main types [1], [2]: 1) the doubly fed induction generator 2) the squirrel cage induction generator 3) the wound rotor synchronous generator and 4) the permanent magnet synchronous generator. Nowadays, the wind energy industry uses PMSG for direct grid-connection because it gives higher efficiency and has no slip ring maintenance. Thus, the lightweight and low maintenance features can be obtained in this type of wind power generation system [3], [4].

The configuration of PMSG wind power generation system is shown in Fig. 1. Presently, there are a few papers examining for the generator-side wind power generation control [5]-[7]. For this reason, this paper focuses on the analysis of the generator-side converter

d-axis stator current control approaches for control of PMSG wind turbines. The generator-side can be controlled with various schemes, the control schemes are separated into three control strategy types to execute different intentions; 1) zero d-axis stator current (ZDSC): control to achieve a linear relationship between the stator current and the generator torque 2) maximum torque per- ampere (MTPA): control to produce maximum generator torque with a minimum stator current and 3) unity power factor (UPF): control to maintain power factor at one. However, there are other techniques for the generator-side control presented in [5]-[6], namely, a vector control. The control strategy in the generator-side has two control loops, three PI controllers and many measured variables from the generator-side and the grid-side which leads to a seriously complicated control design. Compared with the proposed control strategy in [7], ZDSC control can provide a simple topology solution and excellent generator integration performance such as a simple control algorithm, generating maximum efficiency, and minimizing system losses. However, the major drawback of ZDSC control is not suitable for salient-pole synchronous generators and it is not optimal for the operation range over the base speed.

The main objective of this paper is to describe the generator-side performance using ZDSC control scheme. The wind turbine PMSG generation system operates in the base speed range. The dynamic model equations of the PMSG and ZDSC control schemes are analyzed in a space vector diagram and phasor diagram, respectively. The stator power factor and the generator active power are discussed. Furthermore, comparison between the generator active power and the mechanical power are studied to establish a performance enhancement for the system. Additionally, the MPPT method is implemented which can provide the optimal torque control along the whole operation range. Simulation results are shown to verify the performance of the proposed control strategy for PMSG generation system.

## 2. PRINCIPLES OF THE PMSG WIND ENERGY SYSTEM

The configuration of PMSG wind power generation system is shown in Fig. 1. The PMSG converts the mechanical power from the wind turbine into ac electrical power, which is then converted to dc power

Manuscript received on August 27, 2013 ; revised on September 6, 2013.

\* The authors are with Department of Electrical Engineering, Faculty of Engineering, Chiangmai University, Thailand., E-mail: kaengio@gmail.com<sup>1</sup> and yt@eng.cmu.ac.th<sup>2</sup>.

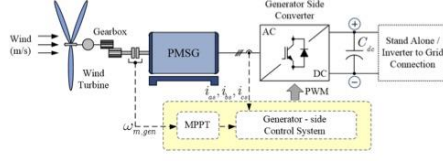


**Fig. 1:** Configuration of PMSG system with control of generator-side converter using  $d$ -axis stator current control scheme.

through a converter with dc link supplying either the stand-alone load or the inverter to a grid-connection. By using an additional inverter, the PMSG can supply the ac electrical power with constant voltage and frequency to the power grid. Two control functions are implemented on the generator-side: one is to extract the maximum power available from the wind turbine and the other is to optimize generator operation, which will be discussed in the following description.

### 2.1 Maximum Power Point Tracking (MPPT) with Optimal Torque Control

The mechanical torque  $T_m$ , which is captured by a wind turbine, can be expressed as [8]

$$T_m = \frac{1}{2} \rho A v_w^3 C_p / \omega_m r_T \quad (1)$$

where  $\rho$  is the air density,  $A$  is the sweep area of the wind turbine  $V_w$ , is the wind velocity,  $r_T$  is the turbine radius,  $\omega_m$  is the generator speed, and  $C_p$  is the power coefficient of the wind turbine.

From (1), in order to capture the maximum mechanical power from a wind turbine at different wind speeds, see the wind turbine power-speed characteristics and maximum power point operation that are shown in Fig. 2. It can be seen that the trajectory of the black circles represents a MPPT power curve, which can be expressed in the term of the mechanical torque  $T_{m,MPPT}$  by the following equations

$$T_{m,MPPT} = K_{opt} \omega_m^2 \quad (2)$$

where  $K_{opt}$  is the coefficient for the optimal torque, which can be calculated according to the rated parameters of the generator.

### 2.2 Dynamic Model of PMSG

In order to get a dynamic model for the PMSG that easily allows us to define the generator-side control system. Fig. 3 shows an arbitrary dq-axis dynamic model of PMSG in the rotor field synchronous reference frame. The voltage equations of the PMSG are given by

$$v_{ds} = -\left(R_s i_{ds} + L_d \frac{di_{ds}}{dt}\right) + \omega_r L_q i_{qs}, \quad (3)$$

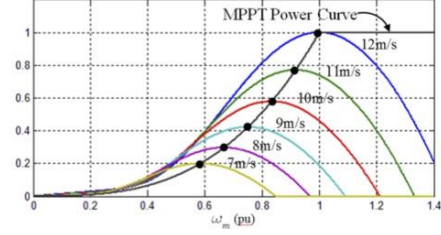


**Fig. 2:** Wind turbine power-speed characteristic and maximum power point tracking method operation.

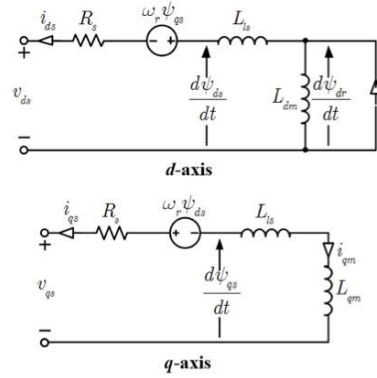


**Fig. 3:** Arbitrary dq-axis dynamic model of the PMSG in the rotor field synchronous reference frame ( $dq$ -axis).

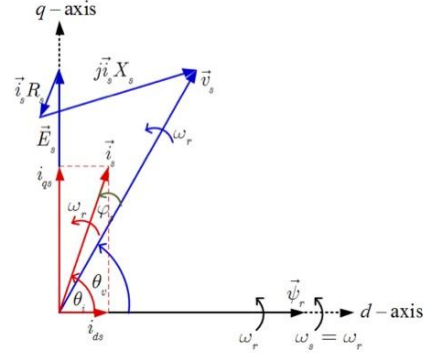


**Fig. 4:** A space vector diagram of the PMSG.

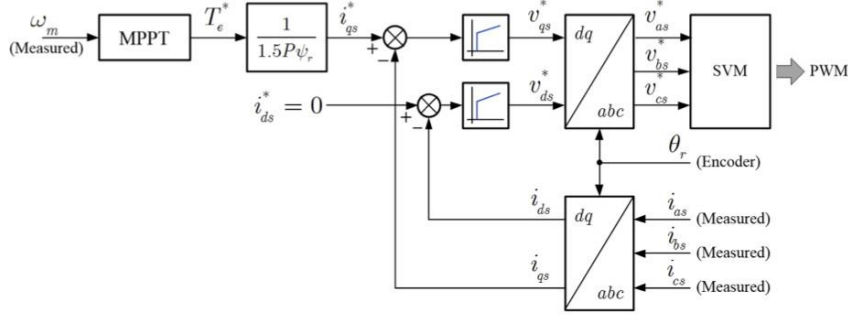


Fig.5: Block diagram of the generator-side control algorithm based on the zero  $d$ -axis stator current control.

$$v_{qs} = -\left(R_s i_{qs} + L_q \frac{di_{qs}}{dt}\right) - w_r L_d i_{ds} + w_r \vec{\psi}_r, \quad (4)$$

where  $R_s$  is the PMSG stator resistance,  $\vec{\psi}_r$  is the rotor flux-linkages,  $L_d$  and  $L_q$  are the stator  $dq$ -axis self-inductances,  $i_{ds}$  and  $i_{qs}$  are the  $dq$ -axis stator currents, and  $w_r$  is rotor speed.

The generator torque  $T_e$  of the PMSG can be calculated by

$$T_e = \frac{3P_p}{2} \left[ \vec{\psi}_r i_{qs} - (L_d - L_q) i_{qs} i_{ds} \right], \quad (5)$$

where  $p_p$  is the pole pairs.

Following the arbitrary  $dq$ -axis dynamic model of the PMSG in Fig. 3, a space vector diagram for the PMSG is expressed in Fig. 4. The space vector diagram is derived under the rotor flux-linkage which is aligned with the  $d$ -axis of the synchronous reference frame. All vectors in this diagram together with  $dq$ -axis frame rotate in space at the synchronous speed, which is also the rotor speed of the generator  $w_r$ .

### 3. CONTROL OF THE GENERATOR-SIDE CONVERTER

#### 3.1 Zero $d$ -axis Stator Current (ZDSC) Control

The proposed generator-side control scheme is shown in Fig. 5. MPPT and ZDSC controls are implemented on the generator-side. The generator torque reference  $T_e^*$  is generated by the MPPT method in agreement with the measured generator speed  $w_m$ . The generator torque reference produces  $q$ -axis stator current reference  $i_{qs}^*$ . The  $d$ -axis generator current reference  $i_{ds}^*$  is set according to the generator operation requirements. The measurement of the three-phase stator currents  $i_{as}, i_{bs}, i_{cs}$  are transformed into  $dq$ -axis stator currents  $i_{ds}, i_{qs}$  according to the measured rotor flux angle  $\theta_r$ . The measured  $dq$ -axis stator currents are subtracted with their current reference. The errors are sent to PI controllers

which lead to obtaining the  $dq$ -axis reference voltages  $v_{ds}^*, v_{qs}^*$  for the converter. The  $dq$ -axis reference voltage  $v_{ds}^*, v_{qs}^*$  are transformed into three-phase reference voltages  $v_{as}^*, v_{bs}^*, v_{cs}^*$  and sent to the PWM generation block using SVM modulation. The proposed generator-side control will be discussed in more detail in the following.

Zero  $d$ -axis stator current control is applied to improve the efficiency of the machine. With this control, the  $d$ -axis stator current component  $i_{ds}$  is then controlled to be zero ( $i_{ds} = 0$ ) to minimize the generator current and thereby reduce the winding losses. With the  $d$ -axis stator current kept at zero, the stator current is equal to its  $q$ -axis component  $i_{qs}$  is

$$i_s = \sqrt{(i_{ds})^2 + (i_{qs})^2} = i_{qs}. \quad (6)$$

According to the ZDSC Control scheme, the generator torque  $T_e$  from (5) can be simplified to

$$T_e = \frac{3}{2} p_p \psi_r i_{qs} = \frac{3}{2} p_p \psi_r i_s. \quad (7)$$

Thus, the  $q$ -axis stator current reference  $i_{qs}^*$  can be determined as the following

$$i_{qs}^* = \frac{T_e^*}{1.5 p_p \psi_r} \quad (8)$$

Considering the relation stated on (7) and (8), the generator torque generated by the  $q$ -axis stator current reference and the generator torque can also be controlled directly by the  $q$ -axis stator current. Furthermore, the  $dq$ -axis reference voltages for the converter can be derived from (3) and (4) as

$$v_{ds}^* = v_{ds}' + w_r L_q i_{qs}, \quad (9)$$

$$v_{qs}^* = v_{qs}' - w_r L_d i_{ds} + w_r \vec{\psi}_r. \quad (10)$$

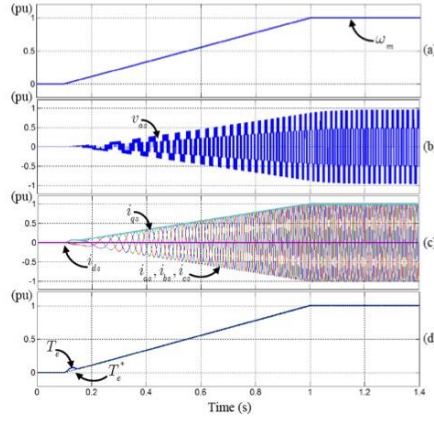






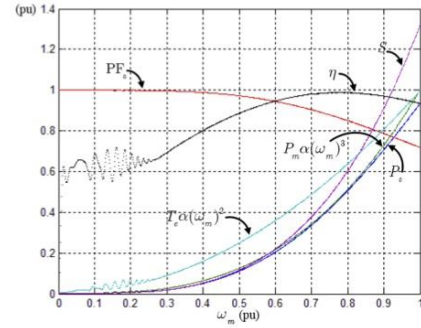
**Table 1:** Permanent magnet synchronous generator parameters

| Permanent Magnet Synchronous Generator Parameters |        |        |      |          |
|---|--------|--------|------|----------|
|   | Real   | Base   |      | Per-unit |
| Rated Mechanical Power                            | 2.448  | 2.448  | MW   | 1.0      |
| Rated Apparent Power                              | 3.419  | 3.419  | MVA  | 1.0      |
| Rated Phase Voltage                               | 2309.4 | 2309.4 | V    | 1.0      |
| Rated Stator Current                              | 490    | 490    | A    | 1.0      |
| Rated Stator Frequency                            | 53.33  | 53.33  | Hz   | 1.0      |
| Rated Rotor Speed                                 | 400    | 400    | rpm  | 1.0      |
| Number of Pole Pairs                              | 8      |        |      |          |
| Rated Mechanical Torque                           | 58.459 | 58.459 | kN.m | 1.0      |
| Rated Rotor Flux-Linkage                          | 4.971  | 6.891  | Wb   | 0.7213   |
| Stator Winding Resistance                         | 24.21  | 4655.7 | mΩ   | 0.0052   |
| <i>d</i> -Axis Stator Inductance                  | 9.816  | 13.965 | mH   | 0.7029   |
| <i>q</i> -Axis Stator Inductance                  | 9.816  | 13.965 | mH   | 0.7029   |

**Fig. 7:** Simulation results of the PMSG with ZDSC control schemes under ramp-startup conditions. (a) generator speed, (b) phase stator voltage, (c) *dq*-axis stator currents and phase stator currents, and (d) generator torque.

shown in Fig. 7(d). With the ZDSC control scheme, the *d*-axis stator current is kept at zero and the response of the *q*-axis stator current doesn't affect the *d*-axis stator current response. In addition, the *q*-axis stator current is proportional to the generator torque.

Fig. 8 shows the performance of the PMSG with the purposed control scheme under the start-up conditions. When the generator speed  $\omega_m$  increases to 0.8 pu, the PMSG reaches 0.99 pu efficiency  $\eta$  and slightly fall to 0.95 pu whilst the generator speed increases to the base speed. In contrast, the stator power factor  $PF_s$  showed different changes by decreasing steadily from 1 pu to 0.71 pu. According to the increase of the appearance power  $S$  to com-

**Fig. 8:** Performance of the PMSG with ZDSC control scheme under start-up conditions.

pensate the generator torque  $T_e$  and active power  $P_s$  around the base speed range, reduction of the PMSG efficiency is occurring at the same time.

Fig. 9 shows the simulated waveforms of the PMSG during the wind speed  $v_w$  step change. Wind speed is assumed to have a stepped-up from 3.6 m/s to 12 m/s at 0.1s and fell sharply to 6 m/s at 0.5sec and then rose slightly reaching around 7.8 m/s at 0.9s. Lastly, wind speed decreased steadily to 4.8 m/s at 1s then remained stable as shown in Fig. 9(a). On the other hand, the wind speed is proportional to the generator speed according to a gearbox ratio Fig. 9(b) and (c) shows the transient waveforms of the stator voltage (phase *a*), stator currents and *dq*-axis stator currents, respectively. Fig. 9(d) shows the optimal reference torque for MPPT and the generator torque. The generator torque follows the optimal reference torque excellently in transient and steady states.

The transient of the mechanical power  $P_m$  and generator active power  $P_s$  are shown in Fig. 9(e).

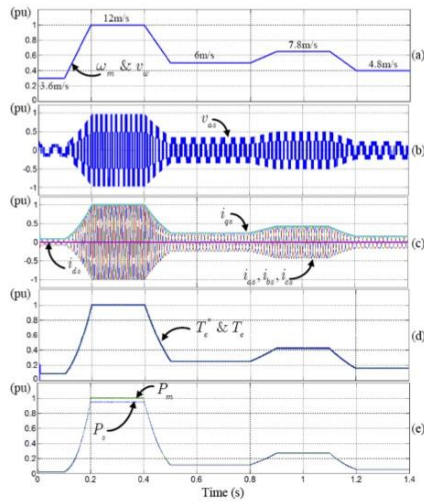


**Fig.9:** Simulation results of the PMSG with ZDSC control scheme under wind speed step changes condition. (a) wind and rotor speed, (b) phase stator voltage, (c) dq-axis stator currents and phase stator currents, (d) generator torque, and (e) generator active power and mechanical power.

At the instant time when the wind speed steps up, the MPPT operation gives the demand for generator torque to increase. The increase of generator torque leads to a higher mechanical power output. As the speed rises up to the base speed, the generator's active power increases, as well. The generator's active power reaches a high point at 0.95 pu. Its winding loss show a 5% (0.05 pu) reduction in power. In contrast, during the wind speed step down transient, the generator torque is first reduced. At the speed slowdown from a base speed of 7 m/s at 0.4s, the generator's active power fall, accordingly and kept constant at a steady state of operation. The mechanical power and the generator's active power almost have the same value, due to a very small winding loss in the machine. Consequently, it is verified that the proposed control scheme can realize high efficiency performance from 0 pu to base speed range, especially in the mid-operational range.

## 5. CONCLUSIONS

In this paper, a performance enhancement of PMSG systems with control of the generator-side converter using  $d$ -axis stator current controller was proposed and its performance was analysed. The control strategy was developed for the optimized generator operation whilst extracting the maximum power from

wind. The proposed control system decouples the  $d$ -axis and  $q$ -axis stator current control through vector control for the generator-side converter. Particularly, the generator current was minimized to reduce the machine winding losses for the achievement of maximum overall performance and efficiency. The operating principles and theoretical analysis were verified using simulation results that exhibited improved high performance and high efficiency.

## ACKNOWLEDGEMENTS

The work was supported by the Faculty of Engineering, Chiang Mai University.

## References

- [1] Z. Chen, J. M. Guerrero, and F. Blaabjerg, "A review of the state of the art of power electronics for wind turbines," *IEEE Trans. Power Electron.*, vol. 24, no.8, pp. 1859-1875, Aug. 2009.
- [2] J. M. Carrasco, L. G. Franquelo, J. T. B. Siewicz, E. Galvan, R. C. P. Guisado, A.M. Parts, J. I. Leon, and N. Moreno-Alfonso, "Power- electronic systems for the grid integration of renewable energy sources: A survey," *IEEE Trans. Ind. Electron.*, vol. 53, no. 4, pp. 1002-1016, Aug. 2006.
- [3] A. Grauers, "Efficiency of three wind energy generator systems," *IEEE Trans. Energy Convers.*, vol. 11, no. 3, pp. 650-657, Sept. 1996.
- [4] Z. Chen, and E. Spooner, "Wind turbine power converters: a comparative study," *Proc. 1998 IEE Power Electron. Variable Speed Drives Seventh Int. Conf.*, 1998, pp. 471-476.
- [5] M. Chinchilla, S. Arnaltes, and J. C. Burgos, "Control of permanent-magnet generators applied to variable-speed wind-energy systems connected to the grid," *IEEE Trans. Energy Convers.*, vol. 21, no. 1, pp. 130-135, Mar. 2006.
- [6] K. Huang, S. Huang, F. She, B. Luo, and L. Cai, "A control strategy for direct-drive permanent-magnet wind-power Generator using back-to-back PWM converter," *ICEMS Conf.*, 2008, pp. 2283-2288.
- [7] S. Zhang, K. Tseng, D. M. Vilathgamuwa, and T. D. Nguyen, "Design of a robust grid interface system for PMSG-based wind turbine generators," *IEEE Trans. Ind. Electron.*, vol. 58, no. 1, pp. 316-328, Jan. 2011.
- [8] E. Koutroulis and K. Kalaitzakis, "Design of a maximum power tracking system for wind-energy-conversion applications," *IEEE Trans. Ind. Electron.*, vol. 53, no. 2, pp. 486-494, Apr. 2006.



**Kitsanu Bunjongjit** received a B.Eng. degree in Electrical engineering from Chiang Mai University, Chiang Mai, Thailand, in 2012, where he is currently studying toward the M.Eng. degree, with a scholarship from the faculty of engineering, Chiang Mai University. His research is focused on electrical drives and renewable energy systems.



**Yuttana Kumsuwan** received a M.Eng. degree in Electrical engineering from King Mongkut's Institute of Technology Ladkrabang, Bangkok, Thailand, in 2000 and a Ph.D. degree in Electrical engineering from Chiang Mai University, Chiang Mai, Thailand, in 2007. Since 2011, he has been an Assistant Professor in the Department of Electrical Engineering, Chiang Mai University. He was a visiting professor at Texas A& M University, College Station, United States, from October 2007 to May 2008, and at Ryerson University, Toronto, ON, Canada from March to May 2010. His research interests include power electronics, energy conversion systems, and electrical drives.



**iEECON 2014**  
 The 2014 International Electrical Engineering Congress  
 March 19-21, 2014, Pattaya City, Thailand



| > Important Dates                          |                    |
|--|--------------------|
| Special session proposal deadline:         | August 30, 2013    |
| Special session notification:              | September 13, 2013 |
| Paper submission extended deadline:        | October 13, 2013   |
| Paper acceptance notification (Postponed): | November 15, 2013  |
| Camera-ready submission extended deadline: | December 20, 2013  |
| Early-bird registration extended deadline: | December 20, 2013  |
| Conference dates:                          | March 19-21, 2014  |

**Welcome to iEECON2014**

The 2014 International Electrical Engineering Congress (iEECON2014) is the second year premier international conference organized by EEAAT, the Electrical Engineering Academic Association (Thailand). In comparison with the first iEECON last year, this year conference shows a rapid growth in terms of not only the number of papers and participants but also the debut of industry technology in the technical session. In addition, good quality papers published in the Proceedings of iEECON2014 will be submitted for inclusion into IEEE Xplore.

On behalf of the Electrical Engineering Academic Association (Thailand), EEAAT, and the organizing committee, we would like to deeply express our sincere appreciation for all participations, both in academics and industry, who play important roles on the great effort and their contributions to the conference. To get achieve at this point, all technical program committee members and voluntary reviewers have worked very hard. Without their cooperati this event would not have been successfully possible. The great appreciation must be address for them. Special thanks also go to the keynote speakers, invited speakers, authors, and sponsors for strongly supporting the conference.

Finally, welcome everyone to the conference. We hope you find iEECON2014 be a good opportunity to meet people and make yourself known by exchanging experiences in both tech and non-technical information. Please enjoy Pattaya as a good place to break up your hard-working days and to refresh your energy for the future experience.



IEEE Catalog Number : 32811



**Assoc. Prof. Dr. Athikom Roeksabutr**  
 iEECON2014 General Chair  
 EEAAT President

**Sponsored By**

Total Solution For Grounding & Lightning Protection  
 as Foundation of Power Quality and Our Safety



# MATLAB/Simulink Modeling of Stator Current Control of PMSG for Grid-Connected Systems

K. Bunjongjit

Department of Electrical Engineering  
Faculty of Engineering, Chiang Mai University  
Chiang Mai 50200, Thailand  
kaengio@gmail.com

Y. Kumsuwan

Department of Electrical Engineering  
Faculty of Engineering, Chiang Mai University  
Chiang Mai 50200, Thailand  
yt@eng.cmu.ac.th

**Abstract**—This paper presents a modeling of stator current control of PMSG for grid-connected systems. The modeling of the power circuit and control-side are performed and represented by using MATLAB/Simulink software to predict and investigate the system operation and the system's dynamic response. Zero- $d$  axis stator current control is implemented to optimize the PMSG for the generator-side converter. The grid-side control scheme decouples active and reactive-power thought voltage-oriented control for the grid-side converter independently. The simulation results are demonstrated to provide the performance and stability of the grid-connected PMSG in the dynamic and steady-state conditions.

**Index Terms**—Permanent-magnet synchronous generator (PMSG), wind power conversion,  $d$ -axis stator current control, voltage-oriented control, modeling

## I. INTRODUCTION

Nowadays, wind power is the most rapid growing renewable energy source. The permanent magnet synchronous generator (PMSG) is mostly applied for variable-speed wind energy conversion system (WECS) because of the higher efficiency and it has no slip ring maintenance. Thus, the features of its lightweight and low maintenance can be obtained in this type of the machine [1]-[2]. In general, the WECS control schemes can be separated into two control-sides, the generator-side and the grid-side control schemes. The generator-side can be controlled with various schemes in [3]-[4]. Corresponding to the grid-side control schemes as well in [5]-[6]. The configuration of PMSG-based WECS with control of the generator-side and grid-side is shown in Fig. 1. A good introduction to the operational characteristics of the PMSG connected to the utility grid can be found in [4]-[6]. It decouples active and reactive power control through voltage-oriented control and optimizes PMSG control for the grid and generator-side converters independently. However, the modeling analysis is needed to guarantee the experimental accuracy and the effectiveness that is responded. Presently, there are a few papers demonstrating the modeling of the PMSG-based WECS. For this reason, this paper performs the modeling of the PMSG-based WECS grid-connection represented by using the MATLAB/Simulink models.

The main objective of this paper is to describe the PMSG-based WECS connected to the utility grid using zero  $d$ -axis stator current (ZDSC) control and voltage-oriented control (VOC) scheme for the generator and grid-side converter,

respectively. The dynamic model equations of the PMSG, VSC Back-to-back (B2B) converter, and grid are introduced and represented by MATLAB/Simulink modeling. Furthermore, the ZDSC control and VOC control schemes are also discussed in the details and represented by the control algorithm diagrams, respectively. Simulation results are shown to verify the proposed control strategy for PMSG-based WECS connected to the utility grid.

## II. MODELLING OF THE POWER CIRCUIT-SIDE

### A. PMSG

In order to described the PMSG modeling as shown in Fig. 2, the voltage equations of the PMSG are given by [3]

$$\begin{bmatrix} v_{ds} \\ v_{qs} \end{bmatrix} = \begin{bmatrix} -R_s & \omega L_q \\ -\omega L_d & -R_s \end{bmatrix} \begin{bmatrix} i_{ds} \\ i_{qs} \end{bmatrix} + \begin{bmatrix} -L_q di_{ds}/dt \\ \omega \vec{\psi}_r - L_d di_{qs}/dt \end{bmatrix}, \quad (1)$$

where  $R_s$  is the PMSG stator resistance,  $\vec{\psi}_r$  is the rotor flux-linkages,  $L_d$  and  $L_q$  are the stator  $dq$ -axis self-inductances,  $i_{ds}$  and  $i_{qs}$  are the  $dq$ -axis stator currents, and  $\omega$  is rotor speed.

The generator torque  $T_e$  of the PMSG can be calculated by

$$T_e = \frac{3p_p}{2} [\vec{\psi}_r i_{qs} - (L_d - L_q) i_{ds} i_{qs}], \quad (2)$$

where  $p_p$  are the pole pairs.

The model has the following as inputs, the stator voltages  $v_s$ , the rotor speed, and the rotor flux linkages. The outputs are the stator currents  $i_s$ , the rotor speed, and the generator torque. The stator currents are delivered to the VSC B2B converter.

### B. VSC Back-to-Back (B2B) Converter

A block diagram of this power converter is shown in Fig. 1. This topology comprises a double conversion from AC to DC and then from DC to AC. Both converters can operate in rectifier or inverter mode. Thus, a bi-directional power flow can be achieved. The output voltage  $V_{uv}$  as a function of the DC-link voltage and the switching functions  $S$  are [7]

$$\begin{bmatrix} v_u \\ v_v \\ v_w \end{bmatrix} = \frac{V_{dc}}{3} \begin{bmatrix} 2 & -1 & -1 \\ -1 & 2 & -1 \\ -1 & -1 & 2 \end{bmatrix} \begin{bmatrix} S_u \\ S_v \\ S_w \end{bmatrix}, \quad (3)$$

The DC-link current can be expressed as a function of the input currents and the switching function by



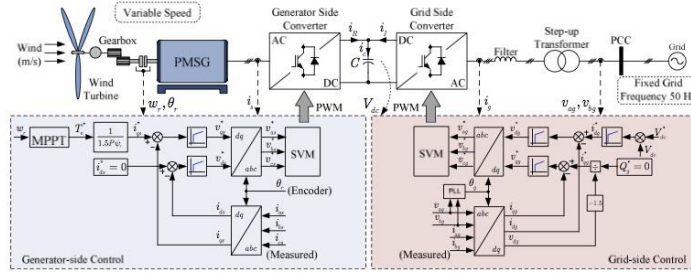


Fig. 1. Configuration of PMSG-based WECS with a control of the generator-side converter using  $d$ -axis stator current control scheme and a control of the grid-side using voltage oriented control scheme.

$$\mathbf{i}_{dq} = \begin{bmatrix} S_a & S_b & S_c \\ i_a \\ i_b \\ i_c \end{bmatrix} \quad (4)$$

Based on (3) and (4), the Simulink model for the VSC has been implemented as shown in Fig 3(a) and 3(c). Typically, the DC-link circuit is represented as an ideal capacitor as shown in Fig. 1. The DC-link voltage, which is the voltage at the capacitor terminals, is given by [7]

$$V_{dc} = \frac{1}{C} \int i_a dt = \frac{1}{C} \int (i_a - i_g) dt, \quad (5)$$

where  $i_g$  is the generator,  $i_a$  is the grid-side converter current, and  $C$  is the capacitor.

In this way the connection between the two considered VSCs can be achieved through the DC-link circuit as shown in Fig. 3. Considering the model of the VSC, the model has as input, the stator  $i_s$  or grid currents  $i_g$ ,  $S$  PWM signal, and DC voltage  $V_{dc}$ . The outputs are the generator or grid-side currents, and the output voltages  $V_{sc}$ . Each of VSC models are connected to the generator and grid-side converter currents together through the DC-link circuit Simulink model.

### C. Grid

The grid can be presented in Fig. 1. The voltage equation per phase can be written as follows

$$v_g = R_g i_g + L_g \frac{di_g}{dt} + v_{pcc}, \quad (6)$$

where  $v_g$  is the grid voltage,  $v_{pcc}$  is the voltage of the PCC bus,  $R_g$  and  $L_g$  are the equivalent impedance that replaces the transformers and the distribution lines.

Considering (6), this equation can be implemented in Simulink software as shown in Fig. 4 using voltage as feedback signal. Furthermore, using of the currents as a feedback signal can also be achieved which depends on the input/output specifications for the model. The inputs are the grid voltages and the voltage of PCC bus. The outputs are the grid currents.

### III. CONTROL-SIDES

The control of the back-to-back converter can be separated in two independent parts with similar structure, in which control of the generator and the grid-side converters as shown

in Fig. 1, respectively. The control of the generator-side employed in a PMSG-based WECS can be established to achieve an optimized generator operation using ZDSC control scheme [3]-[4]. Moreover, the maximum power point tracking (MPPT) with an optimal torque control is also implemented on the generator-side [8] to extract maximum power available from wind turbine. The controller is composed of two independent control loops in the system. They are used to regulate the  $dq$ -axis stator current components with the  $q$ -axis stator current component and utilized to relate the generator torque and  $d$ -axis stator current component which is set to zero according to the generator operation requirement. With this control, the  $d$ -axis stator current component is then controlled to be zero ( $i_{ds} = 0$ ) to minimize the generator current and thereby reduce the winding losses.

The major control functions of the grid-side converter are to regulate the dc-link voltage and manipulate the reactive power output delivered to the grid. The controller is based on grid-voltage orientation control [5]-[6]. Considering the grid-side control algorithm, the controller is composed of three independent control loops in the system, one external loop to control the dc-link voltage and two internal loops to regulate the  $dq$ -axis grid current components, with the  $d$ -axis grid current component utilized to relate the dc-link voltage and the  $q$ -axis grid current component utilized to control the reactive power.

The implementation of two control strategies has been done in Simulink modeling as shown in Fig. 5(a) and 5(b), respectively.

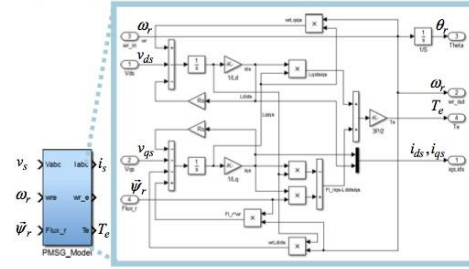


Fig. 2. Simulink model of the permanent magnet synchronous generator (PMSG)

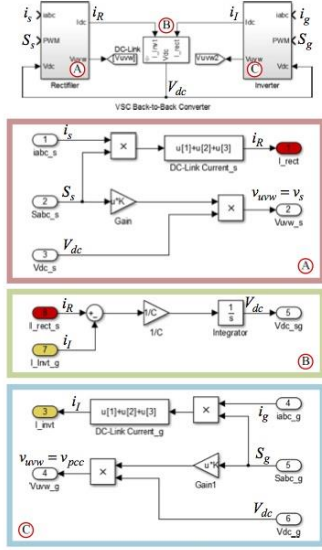


Fig. 3. Simulink model of the VSC back-to-back converter. (a) VSC converter as rectifier mode (b) DC-link circuit and (c) VSC converter as inverter mode.

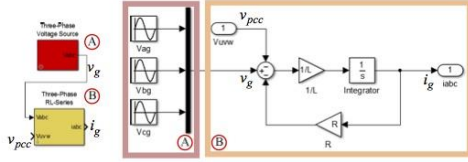


Fig. 4. Simulink implementation of grid model with the voltage as feedback signal. (a) Three-phase voltage source, (b) three-phase RL-series.

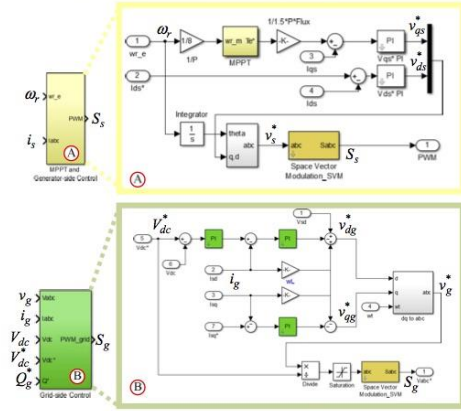


Fig. 5. Simulink model of the control of the generator- and grid-side converter. (a) d-axis stator current control and (b) voltage-oriented control.

#### IV. SIMULATION RESULTS

The PMSG-based WECS operated in grid-connected mode with a control of the generator-side converter using zero  $d$ -axis stator current control scheme and a control of the grid-side using voltage oriented control scheme, as in Fig. 1, is implemented using a MATLAB/Simulink model for the system response and performance simulation. The PMSG parameters are given in Table 1. The simulation results are shown in Fig. 6.

TABLE I. PERMANENT MAGNET SYNCHRONOUS GENERATOR & SYSTEM PARAMETERS

| Permanent Magnet Synchronous Generator Parameters |        |        |                  |          |
|---|--------|--------|------------------|----------|
|   | Real   | Base   |                  | Per-unit |
| Rated Mechanical Power                            | 2.448  | 2.448  | MW               | 1.0      |
| Rated Apparent Power                              | 3.419  | 3.419  | MVA              | 1.0      |
| Rated Phase Voltage                               | 2309.4 | 2309.4 | V <sub>rms</sub> | 1.0      |
| Rated Stator Current                              | 490    | 490    | A                | 1.0      |
| Rated Stator Frequency                            | 53.33  | 53.33  | Hz               | 1.0      |
| Rated Rotor Speed                                 | 400    | 400    | rpm              | 1.0      |
| Number of Pole Pairs                              | 8      |        |                  |          |
| Rated Mechanical Torque                           | 58.459 | 58.459 | kN.m             | 1.0      |
| Rated Rotor Flux-Linkage                          | 4.971  | 6.891  | Wb               | 0.7213   |
| Stator Winding Resistance                         | 24.21  | 4655.7 | mΩ               | 0.0052   |
| $d$ -Axis Stator Inductance                       | 9.816  | 13.965 | mH               | 0.7029   |
| $q$ -Axis Stator Inductance                       | 9.816  | 13.965 | mH               | 0.7029   |
| Grid-side Parameters                              |        |        |                  |          |
| DC-link Voltage reference                         | 7045   | 2309.4 | V                | 3.05     |
| DC-link filter Capacitor                          | 1700   | 425    | μF               | 4.0      |
| Grid Voltage Three-phase Balanced                 | 4000   | 4000   | V <sub>rms</sub> | 1.0      |
| Grid Frequency                                    | 60     | 60     | Hz               | 1.0      |

In the simulation, the turbine model receives the wind speed  $v_w$  and provides an optimized reference torque  $T_e^*$  to control the system. In order to simulate the transient response of the propose control system, wind speed  $v_w$  is assumed to have stepped-up from 3.6 m/s to 12 m/s at 0.2sec and stepped-down to 9 m/s at 0.5sec and then rose slightly reaching around 10.8 m/s at 0.8sec then remained stable. As a result, the optimal reference torque  $T_e^*$  for MPPT is changed accordingly and the generator torque also indicated good dynamics to the tracking responded to its reference, as shown in Fig. 6(a1). With the ZDSC control scheme, in Fig. 6(a2) shows the  $d$ -axis stator current  $i_{ds}$  is kept constant at zero during the  $q$ -axis stator current  $i_{qs}$  is proportional to the generator torque  $T_e$ , which demonstrated good dynamics of the generator-side controller. The electrical dc power  $P_{dc}$  in Fig. 6(a3) showed good tracking to the extracted mechanical power  $P_m$  as the wind step change and the active power  $P_g$  increases. The phase-A stator voltage  $v_{ds}$  and current  $i_{ds}$  is shown in Fig. 6(a4), a leading stator power factor of the generator  $PF_g$  can be obtained due to the proposed control scheme of the generator-side converter. Moreover,  $v_{ds}$  appeared to the constant value according to the constant DC-link voltage  $V_{dc}$  as in Fig. 6(b). The DC-link voltage was maintained at its normal value as the wind speed



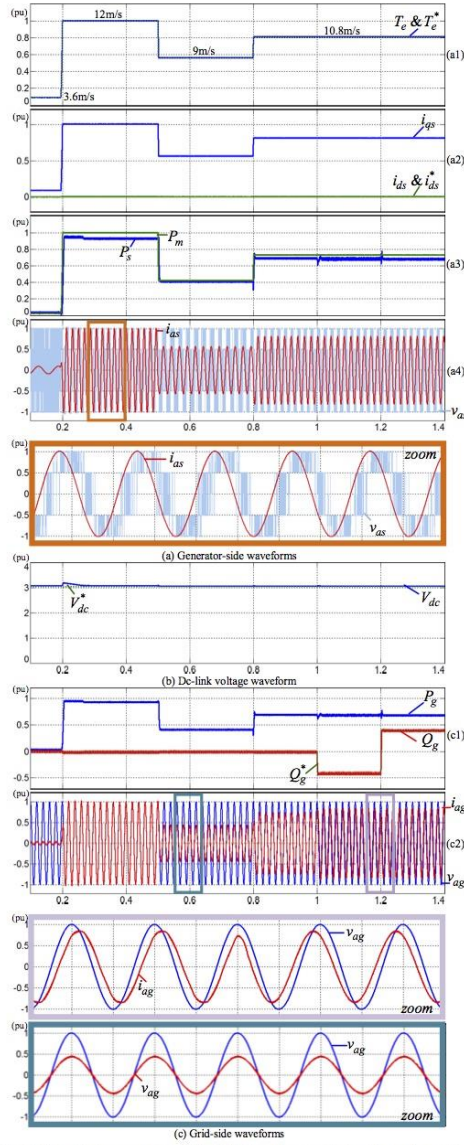


Fig. 6. Simulated waveforms of the PMSG grid-connected with reactive grid power control. (a1) Wind speed, command torque and actual generator torque, (a2) dq-axis stator current and command d-axis stator current, (a3) mechanical power and generator stator power, (a4) phase-A stator voltage and current, (b) dc-link voltage waveform, (c1) command reactive power as well as PMSG-based WECS active and reactive power delivered to the grid, and (c2) phase-A grid voltage and current.

changed due to the effective control of the grid-side converter. The active and reactive powers delivered to grid  $P_g$  and  $Q_g$  shown in Fig. 6(c1),  $P_g$  increases or decreases depends on the the variable wind speed. At  $t = 0.1$ sec, the zero  $Q_g$  was kept unchanged during the transients due to the decoupled control of the active and reactive powers which leads the grid power factor  $PF_g$  to become unified. At  $t = 1$ sec, the reference for the reactive power  $Q_g^*$  start to step from zero to  $-0.45$ pu, demanding a leading grid power factor operation. In contrast, when  $Q_g^*$  step from  $-0.45$  to  $0.45$ pu at  $1.2$ sec indicating a lagging grid power factor operation as well. Fig. 6(c2) shows the phase-A grid voltage  $v_{ag}$  and current  $i_{ag}$ , represent a unity, leading and lagging grid power factor operation.

## V. CONCLUSIONS

In this paper, a modeling of stator current control of PMSG for grid-connected systems was proposed. The modeling of the power circuit and control-side was performed and implemented on the MATLAB/Simulink. Zero  $d$ -axis stator current is used to minimize winding losses of the generator. Thus, optimization of the PMSG was achieved for the generator-side converter. Besides, the voltage-oriented control is used to maintain the DC-link voltage and independent active and reactive-powers flow to the grid. Simulation performances showed fast, accurate, and effective responses to changes in the operating conditions with good dynamics that maintained the demand active and reactive powers to the grid.

## ACKNOWLEDGMENT

The work was supported by the Faculty of Engineering, Chiang Mai University and Energy Conservation Promotion Fund.

## REFERENCES

- [1] A. Grauers, "Efficiency of three wind energy generator systems," *IEEE Trans. Energy Convers.*, vol. 11, no. 3, pp. 650-657, Sep. 1996
- [2] Z. Chen and E. Spooner "Wind turbine power converters: a comparative study," in *Proc. 1998 IEE Power Electronics and Variable Speed Drives Seventh International Conference*, pp. 471-476.
- [3] K. Bunjongjit, and Y. Kumsuwan, "Performance enhancement of PMSG systems with control of generator-side converter using  $d$ -axis stator current controller" *ECTI-CON*, pp. 1-5, May, 2013.
- [4] S. Zhang, K. Tseng, D. Mahinda Vilathgamuwa, and T. D. Nguyen, "Design of a robust grid interface system for PMSG-based wind turbine generators" *IEEE Trans. Ind. Electron.*, vol. 58, no. 1, pp. 316-328, Jan. 2011.
- [5] M. Chinchilla, S. Arnaltes, and J. C. Burgos, "Control of permanent-magnet generators applied to variable-speed wind-energy systems connected to the grid" *IEEE Trans. Energy Convers.*, vol. 21, no. 1, pp. 130-135, Mar. 2006.
- [6] S. A. Saleh, and R. Ahshan, "Resolution-level-controlled WM inverter for PMG-Based wind energy conversion system" *IEEE Trans. Ind. Industry Applications.*, vol. 48, no. 2, pp. 750-763, March 2012.
- [7] F. Iov, A. D. Hansen, P. Sorensen, and F. Blaabjerg, *Wind Turbine Blockset in Matlab/Simulink: General Overview and Description of the Models*. Aalborg University, 2004, no. ISBN 87-89179-46-3.
- [8] E. Koutroulis and K. Kalaitzakis, "Design of a maximum power tracking system for wind-energy-conversion applications," *IEEE Trans. Ind. Electron.*, vol. 53, no. 2, pp. 486-494, Apr. 2006.



# IEEE TENCON-2014 Bangkok, Thailand

22 - 25 October 2014

Leveraging Technology for a Better Tomorrow

IEEE TENCON-2014, Bangkok, Thailand, 22 - 25 October 2014





# An Implementation of Three-level BTB NPC Voltage Source Converter Based-PMSG Wind Energy Conversion System

K. Bunjongjit

Department of Electrical Engineering  
Faculty of Engineering, Chiang Mai  
University, Chiang Mai 50200, Thailand  
kaengio@gmail.com

Y. Kumsuwan

Department of Electrical Engineering  
Faculty of Engineering, Chiang Mai  
University, Chiang Mai 50200, Thailand  
yt@eng.cmu.ac.th

Y. Sriuthaisiriwong

Department of Electrical Engineering  
Faculty of Engineering, Chiang Mai  
University, Chiang Mai 50200, Thailand  
yossanai@eng.cmu.ac.th

**Abstract**—This paper presents an implementation of the three-level back-to-back neutral-point-clamp voltage source converter based PMSG wind energy conversion system (WECS). The generator-side converter performs the maximum power point then tracks, integrates and optimizes control with the  $d$ -axis stator current control (ZDSC), while the grid-side converter regulates the dc-link voltage and reactive power to the grid via voltage oriented control (VOC). An even simple modified unipolar CB-PWM strategy for the three-phase BTB NPC VSC is implemented to simplify the modulation algorithm. The simulation results are demonstrated to provide the performance and stability of the three-level BTB NPC VSC based-PMSG WECS in both the stand-alone and grid-connected conditions.

**Index Terms**—Permanent-magnet synchronous generator (PMSG), wind generation, three-level back-to-back neutral-point-clamp voltage source converter, carrier-based pulse width modulation,  $d$ -axis stator current control

## I. INTRODUCTION

Wind Energy is the most rapid growing renewable energy source. The permanent magnet synchronous generator (PMSG) is mostly applied for the variable-speed wind energy conversion system (WECS) because of the higher efficiency and it has no slip ring maintenance. Thus, the features of its lightweight and low maintenance can be obtained in this type of the machine [1]. The full-scale power converter has recently been increasingly applied in WECS, in a continued effort to increase reliability and improve the efficiency of WECS, a multilevel converter have been developed. Now a day, the multilevel full-scale power converter topologies are dramatically used in medium to high voltage and power industrial applications. Due to the advantages of high power rating and high quality output waveforms connected with reduced current and voltage harmonic distortions, low electromagnetic compatibility (EMC) affects, lower switching losses, lower-common mode voltage, and higher efficiencies when compare with the conventional two-level voltage source converter [2].

The configuration of PMSG-based WECS with control of the generator-side and grid-side is shown in Fig. 1. In general, the WECS control schemes can be separated into two control-

sides, the generator-side and the grid-side control schemes. The generator-side can be controlled with various schemes in [3]-[4], likewise, the grid-side control schemes are in [5]. In order to achieve excellence both in generator-side and grid-side integration performance and a simply algorithm solution, ZDSC and VOC control can provide their required as well. For this reasons, this paper presents an implementation of the three-level back-to-back neutral point clamped voltage source converter based-on WECS integrating with the ZDSC and VOC control for the generator-side and grid-side control, respectively. However, the main drawbacks of the three-level BTB NPC VSC are the greater number of power switches which adds chaos to the modulation technique. Several modulation schemes for the three-level BTB NPC VSC have been expanded [6]. According to the simplicity of implementation, CB-PWM scheme has presumably been the most popular modulation technique based on the comparison between the modulation reference signals and two triangular carriers. On the other hand, in order to facilitate the modulation technique (CB-PWM), only one triangular carrier is employed by using an even simple modified unipolar CB-PWM method [6].

The main objective of this paper is to describe an implementation of the three-level BTB NPC VSC based-PMSG WECS connected to the utility grid using zero  $d$ -axis stator current (ZDSC) control and voltage-oriented control (VOC). The topology configuration of the three-level BTB NPC VSC and the details of the proposed CB-PWM strategy are introduced. Furthermore, the ZDSC and VOC control schemes are also discussed in the details. Simulation results are shown to verify the good performance of the proposed topology and strategy in both of the stand-alone resistive load and grid-connected conditions.

## II. WIND ENERGY CONVERSION SYSTEM

### A. Three-level BTB NPC VSC Configuration

The clarified schematic of the power circuit three-level back-to-back neutral-point-clamped voltage source converter is shown in Fig. 1. Considering on the rectifier side (Blue circle), which compose of 12 active switches, 12 anti-parallel-connected with freewheeling diodes, 6 clamp diodes, and



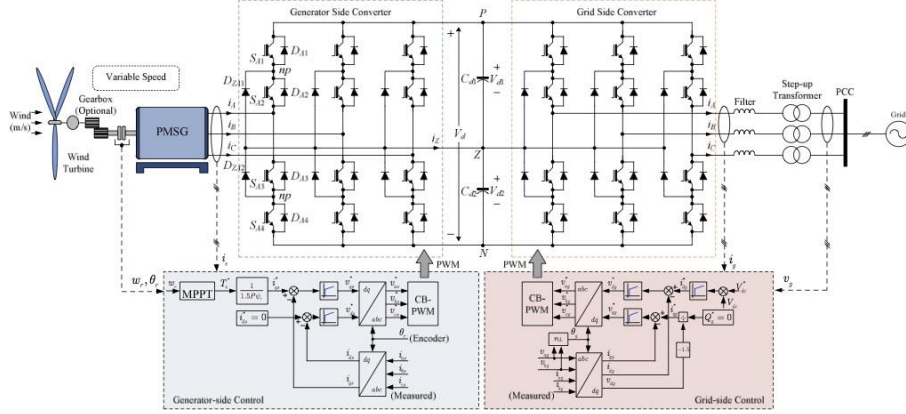


Fig. 1. Clarified schematic of the power circuit three-level back-to-back neutral-point-clamped voltage source converter and the configuration of PMSG-based wind energy conversion system (WECS) with a control of the generator-side converter using  $d$ -axis stator current control scheme and a control of the grid-side using voltage oriented control scheme.

a separate dc-link with series connected capacitors. Demonstrate, the converter leg A is composed of 4 active switched  $S_{A1}$  to  $S_{A4}$  collaborate with 4 anti-parallel-connected with freewheeling diodes  $D_{A1}$  to  $D_{A4}$ . The diodes connected to the neutral point Z,  $D_{ZA1}$  to  $D_{ZA2}$ , are the clamping diodes. On the dc-link side of the converter, the dc-link voltage capacitor is breach into two elements, equipping a neutral point as well.

#### B. Modified Unipolar CB-PWM Strategy

The modified unipolar CB-PWM method [6] is a particularized technique that uses the effective of the three-phase sinusoidal reference voltage  $v_A^*, v_B^*, v_C^*$  and the maximum and minimum of the three reference voltages  $v_{A,M}^*, v_{B,M}^*, v_{C,M}^*$  as

$$v_{A,M}^* = \begin{cases} \frac{v_A^* - \min(v_A^*, v_B^*, v_C^*)}{2} \\ \frac{v_B^* - \min(v_A^*, v_B^*, v_C^*)}{2} \\ \frac{v_C^* - \min(v_A^*, v_B^*, v_C^*)}{2} \end{cases} \quad \text{sgn} \left[ \frac{v_A^* - \max(v_A^*, v_B^*, v_C^*)}{2} + \delta \right] \quad (1)$$

where, sign function (sgn) is defined by +1 or -1, and  $\delta \in \{0,1\}$ .

The modified duty cycles for output pole voltages  $v_{AZ}^*, v_{BZ}^*, v_{CZ}^*$ , that is to divide the dc-link voltage  $V_d$ , can be described as

$$\begin{aligned} d_A &= d_{AP} + d_{AN} = \frac{2v_{AZ}^*}{V_d} \\ d_B &= d_{BP} + d_{BN} = \frac{2v_{BZ}^*}{V_d} \\ d_C &= d_{CP} + d_{CN} = \frac{2v_{CZ}^*}{V_d} \end{aligned} \quad (2)$$

where,  $d_{AP}, d_{BP}, d_{CP}$  are positive duty cycles,  $d_{AN}, d_{BN}, d_{CN}$  are negative duty cycles of the modified duty cycles, and  $d_{AP}, d_{AN}$  are the modified upper and lower duty cycles, respectively.

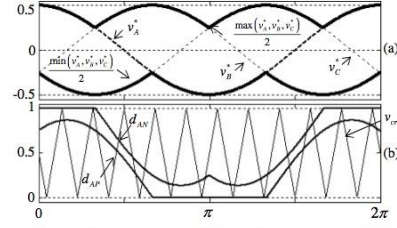


Fig. 2. The modified duty cycles for leg A of the proposed CB-PWM method under the condition of  $m_u = 1.0$ ,  $\text{sgn} = +1$ , and  $\delta = +1$ .

Fig. 2 shows the modified duty cycles of the proposed CB-PWM method. The prototype sinusoidal modulation signals  $v_A^*, v_B^*, v_C^*$  are used to generate the modified duty cycles in the proposed method as shown in Fig. 2(a). In Fig. 2(b) shows the modified duty cycle waveforms  $d_{AP}$  and  $d_{AN}$  for leg A

available from the equation of (1a) and (1b) to a sinusoidal set of balanced modulation signals, which a line period,  $m_a = 1.0$ ,  $\text{sgn} = +1$ , and  $\delta = +1$ . The duty cycles for phase *B* and *C* are the same but phase shifted by  $\pm 2\pi/3$ . From these figures, it can be shown that the waveforms of the modified duty cycles in phase *A* comparative with single triangular wave, which are in the range from 0 to 1. The expression for the modified duty cycle  $d_{AN}$  is the same as  $d_{AP}$  but inverted and phase shifted of  $\pi$  radian.

### III. CONTROL SYSTEM FOR PROPOSE PMSG WECS

The control of the three-level back-to-back neutral-point-clamped voltage source converter can be separated in two independent parts with similar structure, in which the control of the generator and the grid-side converters are shown in Fig. 1, respectively.

#### A. Zero *d*-axis Stator Current (ZDSC) Control for the Generator-side Converter

The control of the generator-side employed in a PMSG-based WECS can be established to achieve an optimized generator operation using ZDSC control scheme [3]-[4]. Moreover, the maximum power point tracking (MPPT) with an optimal torque control is also implemented on the generator-side [4] to extract maximum power available from the wind turbine. The controller is composed of two independent control loops in the system. They are used to regulate the *dq*-axis stator current components  $i_{ds}^*$ ,  $i_{qs}^*$  with the *q*-axis stator current component  $i_{qs}$  and utilized to relate to the generator torque  $T_e$  and *d*-axis stator current component which is set to zero according to the generator operation requirement. With this control, the *d*-axis stator current component is then controlled to be zero [ $i_{ds} = 0$ ] to minimize the generator current and thereby reduce the winding losses, the stator current is equal to its *q*-axis component  $i_{qs}$  is

$$i_s = \sqrt{(i_{ds})^2 + (i_{qs})^2} = i_{qs}. \quad (3)$$

According to the ZDSC control scheme, the generator torque [6] can be simplified to

$$T_e = \frac{3}{2} p_s \psi_s i_{qs} = \frac{3}{2} p_s \psi_s i_s. \quad (4)$$

Thus, the *q*-axis stator current reference  $i_{qs}^*$  can be determined as the following

$$i_{qs}^* = \frac{T_e^*}{1.5 p_s \psi_s}. \quad (5)$$

Considering the relation stated on (4) and (5), the generator torque generated by the *q*-axis stator current reference and the generator torque can also be controlled directly by the *q*-axis stator current. A step-by-step procedure for the generation of PWM gating signal is given as follows:

- 1) The reference torque  $T_e^*$  is originated by the MPPT algorithm in accordance with the measured wind

speed  $\omega_m$ . The torque reference producing stator current  $i_{qs}^*$  is calculated from  $T_e^*$  as equation (4)

- 2) The *d*-axis stator current reference  $i_{ds}^*$  is arranged to zero [ $i_{ds} = 0$ ] to achieve the ZDSC control method. For rotor flux position, the rotor flux positioning angle  $\theta_r$  can be detected by a speed encoder. The measured three-phase stator currents  $i_{as}, i_{bs}, i_{cs}$  are transformed into the *dq*-axis stator currents  $i_{ds}, i_{qs}$ .
- 3) The measured *dq*-axis stator currents are then compared with their own reference currents  $i_{ds}^*, i_{qs}^*$ . The errors are sent to two PI controllers, which generated the *dq*-axis reference voltages  $v_{ds}^*, v_{qs}^*$ , for the generator-side converter. These two synchronous-frame reference voltages are then transformed to three-phase reference voltages  $v_{as}^*, v_{bs}^*, v_{cs}^*$ .
- 4) The three-phase reference voltages are sent to the PWM generation block algorithm. Either modified unipolar CB-PWM modulation techniques can be employed as already discussed in the previous section.

The generator-side (rectifier) input voltages which are likewise the generator stator voltages, can then be varies according to their references values such that the generator active power controlled.

#### B. Voltage-Oriented-Control (VOC) for the Grid-side Converter

The major control functions of the grid-side converter are to regulate the dc-link voltage and manipulate the reactive power output delivered to the grid. The controller is based on the grid-voltage orientation control [5]. Considering the grid-side control algorithm, the controller is composed of three independent control loops in the system, one external loop to control the dc-link voltage and two internal loops to regulate the *dq*-axis grid current components, with the *d*-axis grid current component utilized to relate the dc-link voltage and the *q*-axis grid current component utilized to control the reactive power. To achieve the VOC control scheme, the *d*-axis of the synchronous frame is aligned with the grid voltage vector, therefore the *d*-axis grid voltage is equal to its magnitude [ $v_{dg} = v_g$ ], and the resultant *q*-axis voltage is then equal to zero [ $v_{qg} = \sqrt{v_g^2 - v_{dg}^2} = 0$ ]. The active power and reactive power of the system can be express as

$$P_e = \frac{3}{2} v_{dg} i_{dg}, \quad (6)$$

$$Q_e = -\frac{3}{2} v_{dg} i_{qg}. \quad (7)$$

The *q*-axis current reference can then be obtain from

$$i_{qg}^* = \frac{Q_e^*}{-1.5 v_{dg}}, \quad (8)$$

where  $Q_e^*$  is the reactive power reference, which might be set to zero for the unity power factor operation [7].

#### IV. SIMULATION RESULTS

In this section, the PMSG-based WECS topology and control scheme are simulated in MATLAB/Simulink. They are operated in stand-alone resistive load and grid-connected mode. The PMSG and the system parameters are given in Table 1. The simulation results are shown in Figs. 3-4.

TABLE I. PERMANENT MAGNET SYNCHRONOUS GENERATOR & SYSTEM PARAMETERS

| Permanent Magnet Synchronous Generator Parameters |        |        |      |          |
|---|--------|--------|------|----------|
|   | Real   | Base   |      | Per-unit |
| Rated Mechanical Power                            | 2.448  | 2.448  | MW   | 1.0      |
| Rated Apparent Power                              | 3.419  | 3.419  | MVA  | 1.0      |
| Rated Phase Voltage                               | 2309.4 | 2309.4 | Vrms | 1.0      |
| Rated Stator Current                              | 490    | 490    | A    | 1.0      |
| Rated Stator Frequency                            | 53.33  | 53.33  | Hz   | 1.0      |
| Rated Rotor Speed                                 | 400    | 400    | rpm  | 1.0      |
| Number of Pole Pairs                              | 8      |        |      |          |
| Rated Mechanical Torque                           | 58.459 | 58.459 | kN.m | 1.0      |
| Rated Rotor Flux-Linkage                          | 4.971  | 6.891  | Wb   | 0.7213   |
| Stator Winding Resistance                         | 24.21  | 4655.7 | mΩ   | 0.0052   |
| <i>d</i> -Axis Stator Inductance                  | 9.816  | 13.965 | mH   | 0.7029   |
| <i>q</i> -Axis Stator Inductance                  | 9.816  | 13.965 | mH   | 0.7029   |
| Grid-side Parameters                              |        |        |      |          |
| DC-link Voltage ref.                              | 7045   | 2309.4 | V    | 3.05     |
| DC-link filter Capacitor                          | 1700   | 425    | μF   | 4.0      |
| Grid Voltage Three-phase Balanced                 | 4000   | 4000   | Vrms | 1.0      |
| Grid Frequency                                    | 60     | 60     | Hz   | 1.0      |

In order to simulate the transient response of the propose control system, Fig. 3 shows the simulated waveforms of the PMSG in the stand-alone condition during the wind speed step change. Wind speed  $v_w$  is assumed to have stepped-up from 3.6 m/s to 12 m/s at 0.2sec and stepped-down to 9 m/s at 0.5sec and then rose slightly reaching around 10.8 m/s at 0.8sec then remained stable. As the results, the optimal reference torque  $T_r^*$  for MPPT is changed accordingly and the generator torque also indicated good dynamics to the tracking responded to its reference, as shown in Fig. 3(a). With the ZDSC control scheme, in Fig. 3(b) shows the *d*-axis stator current  $i_{ds}$  is kept constant at zero during the *q*-axis stator current  $i_{qs}$  is proportional to the generator torque  $T_r$ , which demonstrated good dynamics of the generator-side controller. The Dc-link voltage is changed following to the wind speed step changed, due to connecting to the stand-alone resistive load as shown in Fig. 3(c). The transient of the mechanical power  $P_m$  and generator active power  $P_g$  are shown in Fig. 3(d). As the wind speed rises up to the base speed (12 m/s), the generator's active power reaches a high point at 0.95 pu. It's winding loss show a 5% (0.05 pu) reduction in power. In contrast, during the wind speed decrease from a base speed to 9 m/s at 0.5sec, the mechanical power and the generator's active power almost have the same value due to a very small winding loss in the machine. The phase-A stator voltage  $v_{as}$  and current  $i_{as}$  is shown in Fig. 3(e), a leading stator power factor of the generator  $PF_s$  can be obtained according to the proposed control scheme of the generator-side converter.

Fig. 4 shows the simulated waveforms of the PMSG operated under the grid-connected condition during the wind speed step change. It's assumed to have the wind speed step changed as the same condition following to the previous condition (Stand-alone). Fig. 4(a) performed the excellent dynamic response of the generator torque  $T_e$ . As the proposed control scheme, the *d*-axis stator current is remaining constant at zero while the *q*-axis stator current is changing accordingly as shown in Fig. 4(b). The phase-A stator voltage  $v_{as}$  and current  $i_{as}$  is shown in Fig. 4(c).  $v_{as}$  appeared to the constant value according to the constant DC-link voltage  $V_{dc}$  as in Fig. 4(d). The DC-link voltage was maintained at its normal value as the wind speed changed due to the effective control of the grid-side converter. The mechanical, active and reactive powers are delivered to the grid  $P_m$ ,  $P_g$  and  $Q_g$  as shown in Fig. 4(e),  $P_m$  and  $P_g$  are increased or decreased depending on the variable wind speed. According to the grid-side control scheme,  $Q_g$  is keep at zero indicating a unity grid power factor as well. Fig. 4(f) shows the phase-A grid voltage  $v_{og}$  and current  $i_{og}$ , represent a unity grid power factor operation. Moreover, phase- U grid voltage shows a six-step waveform

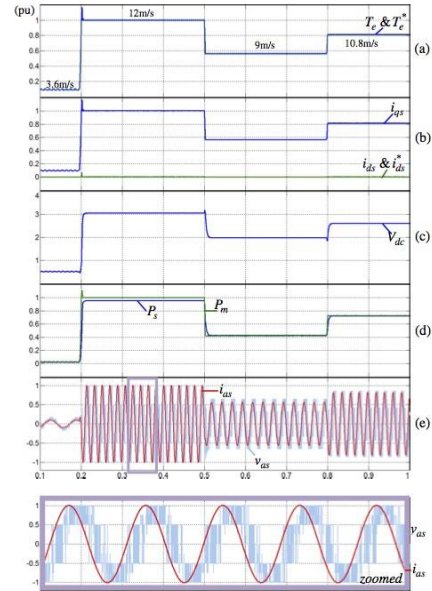


Fig. 3. Simulated waveforms of the PMSG under the stand-alone condition. (a) wind speed, command torque and actual generator torque, (b) *dq*-axis stator current and command *d*-axis stator current, (c) DC-link voltage waveform, (d) mechanical power and generator stator power, (e) phase-A stator voltage



due to use of the NPC Three-level VSC. During the low-switching frequency 1 kHz, grid current appeared to have little distortion. On the other hand, the switching losses in the switching devices are reduced.

In Fig. 5, the characteristic of the PMSG with the propose control scheme under grid-connected condition. The stator power factor  $PF_s$  under the ZDSC control is decreased when the generator speed is increased. While the generator torque  $T_g$ , mechanical power  $P_m$ , grid active power  $P_g$  and the apparent-

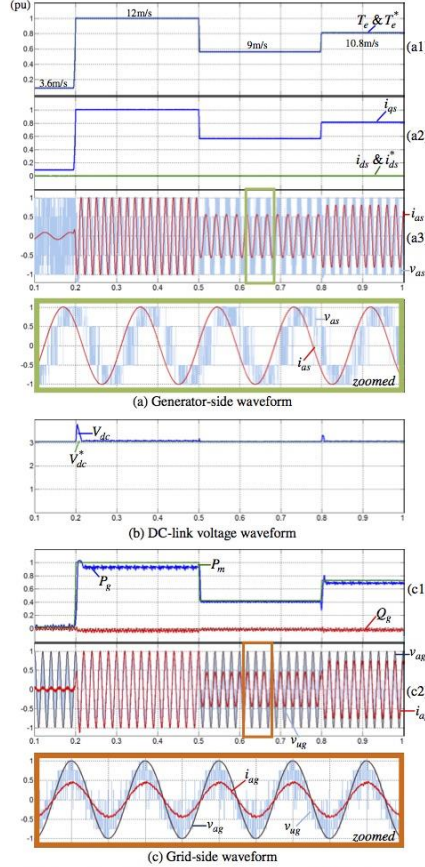


Fig. 4. Simulated waveforms of the PMSG grid-connected. (a1) wind speed, command torque and actual generator torque, (a2)  $dq$ -axis stator current and command  $d$ -axis stator current, (a3) phase-A stator voltage and current, (b) DC-link voltage waveform, (c1) mechanical, active and reactive power and (c2) phase-U grid voltage, phase-A grid voltage, and current.

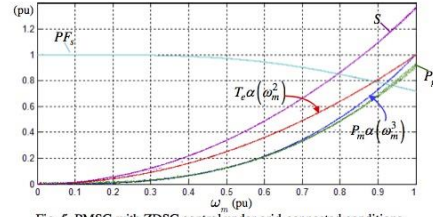


Fig. 5. PMSG with ZDSC control under grid-connected conditions characteristic.

power  $S$  are similarly increased for the entire speed range. According to the increase of the appearance power to compensate  $T_g$  and  $P_g$  around the base speed range, reduction of the PMSG efficiency is occurring at the same time.

## V. CONCLUSIONS

In this paper, an implementation of the three-level back-to-back neutral-point-clamp voltage source converter based PMSG wind energy conversion was proposed. The proposed configuration combines the advantages of the generator-side and the grid-side multilevel operation. Zero  $d$ -axis stator current is used to minimize winding losses of the generator. Thus, optimization of the PMSG was achieved for the generator-side converter whilst extracting the maximum power from wind. Besides, the voltage-oriented control is used to maintain the DC-link voltage and independent active and reactive-powers flow to the grid. An even simple modified unipolar CB-PWM modulation strategy was implemented, which led to a simple PWM algorithm. Through the simulation results both in stand-alone and grid-connected condition, it has been demonstrated that BTB NPC VSC performs very well in achieving the control goals for the complete PMSG wind energy conversion system.

## ACKNOWLEDGMENT

This work was supported by the Faculty of Engineering, Chiang Mai University.

## REFERENCES

- [1] A. Grauers, "Efficiency of three wind energy generator systems," *IEEE Trans. Energy Convers.*, vol. 11, no. 3, pp. 650-657, Sep. 1996
- [2] J. Rodriguez, J. Lai, and F. Peng, "Multilevel inverters: A survey of topologies, controls and applications," *IEEE Trans. Ind. Electron.*, vol. 49, no. 4, pp. 724-738, Aug. 2002.
- [3] S. Zhang, K. Tseng, D. Mahinda Vilathgamuwa, and T. D. Nguyen, "Design of a robust grid interface system for PMSG-based wind turbine generators" *IEEE Trans.*, vol. 58, no. 1, pp. 316-328, Jan. 2011.
- [4] M. Chinchilla, S. Arnaltes, and J. C. Burgos, "Control of permanent-magnet generators applied to variable-speed wind-energy systems connected to the grid" *IEEE Trans.*, vol. 21, no. 1, pp. 130-135, Mar. 2006.
- [5] E. Koutoulis and K. Kalaitzakis, "Design of a maximum power tracking system for wind-energy-conversion applications," *IEEE Trans. Ind. Electron.*, vol. 53, no. 2, pp. 486-494, Apr. 2006.
- [6] W. Srirattanawichaiikul, S. Premrudeeprachacham, and Y. Kumswan, "Modified unipolar carrier-based PWM strategy for three-level neutral-point-clamped voltage source inverters" *J. Electr. Eng. Technol.*, vol. 8, pp. 742-753, Sep. 2013.
- [7] R. Vargas, P. Cortes, U. Ammann, J. Rodriguez, and J. Pontt, "Predictive control of a three-phase neutral-point-clamped inverter," *IEEE Trans. Ind. Electron.*, vol. 54, no. 5, pp. 2697-2705, Oct. 2007.

## ประวัติผู้เขียน

|                   |   |
|-------------------|---|
| ชื่อ-นามสกุล      | นายกฤษฎ วรรณจติตต์  |
| วัน เดือน ปี เกิด | 9 กุมภาพันธ์ 2533   |
| ประวัติการศึกษา   | ปีการศึกษา 2554 สำเร็จการศึกษาวิศวกรรมศาสตรบัณฑิต สาขาวิศวกรรมไฟฟ้า มหาวิทยาลัยเชียงใหม่  |
| ทุนการศึกษา       | ทุนการศึกษาเพื่อศึกษาต่อระดับปริญญาโท เพื่อส่งเสริมความเป็นเลิศทางการวิจัย ประจำปีการศึกษา 2555-2556  |
| ผลงานตีพิมพ์      | 2013 10 <sup>th</sup> International Conference Organized by Electrical Engineering/Electronics, Computer, Telecommunication and Information Technology (ECTI-CON 2013) Association : K. Bunjongjit and Y. Kumsuwan, "Performance Enhancement of PMSG Systems with Control of Generator-side Converter Using d-axis Stator Current Controller," in <i>Proc. IEEE ECTI-CON</i> , 2013.<br>2014 2 <sup>nd</sup> International Electrical Engineering Congress (iEECON 2014) : K. Bunjongjit and Y. Kumsuwan, "MATLAB/Simulink Modeling of Stator Current Control of PMSG for Grid-Connected Systems," in <i>Proc. IEEE iEECON</i> , 2014.<br>2014 Technologies for smart nation (TENCON 2014) : K. Bunjongjit, Y. Kumsawan and Y. Srithaisiriwong, "An Implementation of Three-level BTB NPC Voltage Source Converter Based-PMSG Wind Energy Conversion System," in <i>Proc. IEEE TENCON</i> , 2014. |

